Accepted Manuscript

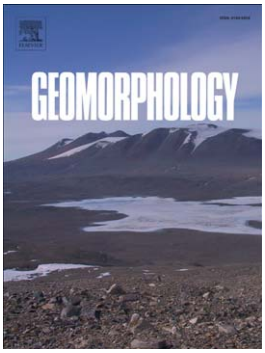

Water erosion susceptibility mapping by applying stochastic gradient treeboost to the imera Meridionale River basin (Sicily, Italy)

Silvia Eleonora Angileri, Christian Conoscenti, Volker Hochschild, Michael Märker, Edoardo Rotigliano, Valerio Agnesi

PII: S0169-555X(16)30108-8
DOI: doi: 10.1016/j.geomorph.2016.03.018
Reference: GEOMOR 5550

To appear in: *Geomorphology*

Received date: 12 January 2015
Revised date: 13 November 2015
Accepted date: 16 March 2016

Please cite this article as: Angileri, Silvia Eleonora, Conoscenti, Christian, Hochschild, Volker, Märker, Michael, Rotigliano, Edoardo, Agnesi, Valerio, Water erosion susceptibility mapping by applying stochastic gradient treeboost to the imera Meridionale River basin (Sicily, Italy), *Geomorphology* (2016), doi: 10.1016/j.geomorph.2016.03.018

This is a PDF file of an unedited manuscript that has been accepted for publication. As a service to our customers we are providing this early version of the manuscript. The manuscript will undergo copyediting, typesetting, and review of the resulting proof before it is published in its final form. Please note that during the production process errors may be discovered which could affect the content, and all legal disclaimers that apply to the journal pertain.

ACCEPTED MANUSCRIPT

Water erosion susceptibility mapping by applying Stochastic Gradient Treeboost to the Imera Meridionale River Basin (Sicily, Italy)

Silvia Eleonora Angileri[a,*], Christian Conoscenti[a], Volker Hochschild[b], Michael Märker [c,d], Edoardo Rotigliano [a], Valerio Agnesi [a]

[a] *Department of Earth and Sea Science (DiSTeM), University of Palermo, Via Archirafi 22, 90123 – Palermo, Italy*

[b] *Institute of Geography, Faculty of Geosciences, Eberhard Karls Universität Tübingen, Rümelinstr. 19-23, 72070 Tübingen, Germany*

[c] *Department of Plant, Soil and Environmental Sciences, University of Florence, Piazzale delle Cascine 14, I-50144 Florence, Italy*

[d] *Heidelberg Academy of Sciences and Humanities, ROCEEH, C/o University of Tübingen, Rümelinstr. 19-23, 72070 Tübingen, Germany*

* Corresponding author.–Tel: +3909123864643; Mobile: +393294221106; Fax: +39 0916169908,

E-mail addresses: silviaeleonora.angileri@unipa.it, silviaangileri@gmail.com (S.E. Angileri)

ACCEPTED MANUSCRIPT

ACCEPTED MANUSCRIPT

Abstract

Soil erosion by water constitutes a serious problem affecting various countries. In the last few years, a number of studies have adopted statistical approaches for erosion susceptibility zonation. In this study, the Stochastic Gradient Treeboost (SGT) was tested as a multivariate statistical tool for exploring, analyzing and predicting the spatial occurrence of rill-interrill erosion and gully erosion. This technique implements the stochastic gradient boosting algorithm with a tree-based method. The study area is a 9.5 km^2 river catchment located in central-northern Sicily (Italy), where water erosion processes are prevalent, and affect the agricultural productivity of local communities. In order to model soil erosion by water, the spatial distribution of landforms due to rill-interrill and gully erosion was mapped and 12 environmental variables were selected as predictors. Four calibration and four validation subsets were obtained by randomly extracting sets of negative cases, both for rill-interrill erosion and gully erosion models. The results of validation, based on receiving operating characteristic (ROC) curves, showed excellent to outstanding accuracies of the models, and thus a high prediction skill. Moreover, SGT allowed us to explore the relationships between erosion landforms and predictors. A different suite of predictor variables was found to be important for the two models. Elevation, aspect, landform classification and land-use are the main controlling factors for rill-interrill erosion, whilst the stream power index, plan curvature and the topographic wetness index were the most important independent variables for gullies. Finally, an ROC plot analysis made it possible to define a threshold value to classify cells according to the presence/absence of the two erosion processes. Hence, by heuristically combining the resulting rill-interrill erosion and gully erosion susceptibility maps, an integrated water erosion susceptibility map was created. The adopted method offers the advantages of an objective and repeatable procedure, whose result is useful for local administrators to identify the areas most susceptible to water erosion and best allocate resources for soil conservation strategies.

1. Introduction

Soil erosion by water constitutes a serious land degradation phenomenon affecting around one billion hectares in the world (Lal, 2003), causing the reduction of vegetation growth, siltation of water courses, filling of valleys and reservoirs, and formation of deltas along coastal areas (Kosmas et al., 1997). Water erosion on hillslopes is generated by rainsplash and overland runoff, mainly taking the form of rill-interril and gully erosion, the former including five individual sub-processes: splash erosion, sheetwash, rainflow, runoff and piping (Bryan, 2000). Their distribution on the slopes is mainly influenced by micro-topography, vegetation, animal tracking and tillage operations

ACCEPTED MANUSCRIPT

(Bryan and Kuhn, 2002). Gully erosion is one of the most complex erosion phenomena (Poesen et al., 2003; Chaplot et al., 2005), most often triggered or accelerated by a combination of inappropriate land use and extreme rainfall events (Valentin et al., 2005). In semi-arid and arid regions, the contribution of gullies to the overall sediment production was estimated to be 50–80% (Poesen et al., 2002). Gully erosion involves a wide range of sub-processes, such as head-cut retreat, piping, fluting, tension crack development and mass wasting (Imeson and Kwaad, 1980). Furthermore, gully evolution has been recognized to occur in subsequent stages: more than 90% of gully length is formed during the first stage of gully initiation (5% of the gully's entire lifetime), while its morphologic conditions are relatively stable during the remaining stages (Sidorchuk, 1999).

As both rill and gully erosion are threshold phenomena (Emmett, 1970; Dunne and Aubry, 1986; Montgomery and Dietrich, 1994), several studies have focused on defining the hydraulic and topographic conditions for predicting the initiation of rills and gullies (Govers et al., 2007). Numerous types of experimental plots and laboratory flumes have been used to identify hydraulic indices for rill initiation and development (Merritt, 1984; Govers, 1985; Govers and Rauws, 1986; Torri et al., 1987; Bryan, 1990; Prosser et al., 1995; Giménez and Govers, 2001; Cerdan et al., 2002; Yao et al., 2008; Wirtz et al., 2012; Di Stefano et al., 2013). Studies showed that the hydraulic indices that most influence rill initiation are: shear velocity (Govers, 1985), stream power (Rose, 1985) and unit stream power (Moore and Burch, 1986). Research on gully erosion thresholds is commonly based on the hypothesis that Hortonian overland flow dominates the gullying process. Indeed, several experiments aimed at predicting gully initiation points use saturation overland flow as a dominant factor (Patton and Schumm, 1975; Foster, 1986; Thorne et al., 1986; Merkel et al., 1988; Auzet et al., 1995). Saturation overland flow mainly depends on two terrain attributes: the upslope drainage area (A_s) and the slope gradient (S). An inverse relationship between these two attributes has been widely used to predict the location and size of gullies (e.g. Moore et al., 1988; Desmet and Govers, 1997; Vandekerckhove et al., 1998). However, several studies have suggested that other factors should be included in gully occurrence models (Montgomery and Dietrich, 1988; Bocco, 1991; Chaplot and Bissonnains., 2003; Poesen et al., 2006). Actually, where Horton overland flow is rare, more processes can be recognized as contributing to gully initiation and development, namely, incision by saturation overland flow, seepage erosion, shallow landsliding and piping (Imeson and Kwaad, 1980).

In addition to a threshold approach, features and locations of soil erosion processes may also be predicted by using bivariate to multivariate statistical techniques. These methods allow an investigator to explain the occurrence of erosion processes, by crossing the spatial distribution of

ACCEPTED MANUSCRIPT

the water erosion landforms (the outcome) with that of a set of geo-environmental variables (the predictors).

In the field of geomorphology, computer-aided statistical methods have been widely adopted to assess landslide susceptibility (e.g. Guzzetti et al., 1999, 2006; Neuhäuser and Terhorst, 2007; Carrara and Pike, 2008; Rossi et al., 2010; Vergari et al., 2011; Marjanović et al., 2011; Pozdnoukhov et al., 2011; Rotigliano et al., 2011; Costanzo et al., 2012; Ballabio and Sterlacchini, 2012; Costanzo et al., 2013; Lombardo et al., 2014, 2015; Conoscenti et al., 2015). An increasing number of studies have also adopted a stochastic approach for zoning water erosion susceptibility. In addition to bivariate analyses (Conoscenti et al., 2008, 2013; Conforti et al., 2010; Magliulo, 2010; Lucà et al., 2011; Magliulo, 2012) different multivariate statistical methods have also been employed to this aim, such as logistic regression (Lucà et al., 2011; Conoscenti et al., 2014), classification and regression trees (Geissen et al., 2007; Gómez Gutiérrez et al., 2009a; Märker et al., 2011), and multivariate adaptive regression splines (Gómez Gutiérrez et al., 2009a,b, 2015).

In the present study, we adopted the Stochastic Gradient Treeboost (SGT, Friedman, 1999) as a multivariate statistical tool for exploring, analyzing and predicting the spatial occurrence of soil erosion processes. SGT integrates the stochastic gradient boosting algorithm (Friedman, 2001) with a tree-based method, which generally results in accurate and robust predictions (Friedman, 2002) with low overfitting effects (Brenning, 2005). Moreover, SGT can work with a variety of independent variables, such as categorical, binary, ordinal or continuous types (Elith et al., 2008). SGT was applied by exploiting the Salford Systems implementation in TreeNet®, using a tree complexity of six nodes and a bag fraction of 0.75. As SGT provides an estimate of the probability of presence for each mapping unit, it is suitable for preparing water erosion susceptibility maps. These show how proneness to erosion changes over an area, providing useful information for establishing land use plans and remediation strategies. However, despite the increasing attention paid to the statistical modeling of erosion susceptibility, relatively few studies have attempted to assess susceptibility conditions for different erosion processes (Flügel et al., 2003; Geissen et al., 2007; Conoscenti et al., 2008; Märker et al., 2011; Magliulo, 2012). The main objectives of this study are: (1) to explore the ability of SGT to predict the spatial occurrence of rill-interrill and gully erosion; (2) to better understand the relationships between these erosion processes and their controlling factors; and (3) to design a methodological approach for preparing combined water erosion susceptibility maps. The study was carried out in a small basin of central-northern Sicily (Italy), where severe soil erosion processes affect the productivity of local agricultural systems. In this area, different statistical methods were employed to predict gully occurrence: Conoscenti et al. (2014) applied the Forward Stepwise Logistic Regression (FSLR) analysis, comparing the

ACCEPTED MANUSCRIPT

performance of grid-cell and slope units based models, while Gómez-Gutiérrez et al. (2015) applied the Multivariate Adaptive Regression Spline (MARS), testing different pixel sizes (2, 4, 10, 20 and 50 m).

2. Materials and methods

2.1. Study area

The study area is the San Giorgio River catchment, which extends for approximately 9.5 km^2 in the head sector of the Imera Meridionale River, one of the main fluvial systems of Sicily (Fig. 1). The elevation ranges from 585 to 1,020 m a.s.l., whereas the mean slope in the area is 11°. The rainfall is mainly concentrated in a few days during autumn and winter, while spring and summer are characterized by dry conditions, with an average yearly precipitation of nearly 700 mm (Conoscenti et al., 2014).

The San Giorgio River catchment is characterized by the wide outcropping of Upper Cretaceous to Lower Messinian clay sediments that occupy almost 90% of the total area. These deposits give rise to gentle slopes, which are only interrupted by morphological steps where less erodible conglomerates (Upper Tortonian-Lower Messinian), gypsum (Messinian) and sandstones (Lower Messinian) crop out. The fluvial network, characterized by an intermittent hydrological regime, develops through a typical rural agricultural landscape, dominated by crops, fruit tree orchards and pastures.

Because of intensive agricultural activities, soils in most of the study area are degraded and compacted. The soils are generally thin and weakly developed (mainly *regosols* and *cambisols*), with a fine-medium texture (Fierotti et al., 1988; Montana et al., 2011); they easily form surface crusts giving rise to the loss of porosity continuity. As a consequence, infiltration is reduced during intense rainfall events, whilst runoff and soil erosion increase.

2.2. Erosional landforms

In light of the widespread presence of a clayey substratum, the morphodynamic activity in the San Giorgio catchment is dominated by gravitational (mud- and debris-flows) and intense water erosion (sheet, rill and gully erosion). By integrating field surveys and visual interpretation of available high-resolution orthophotos (pixel size 0.25 m, year 2007), the water erosional landforms affected by rill-interrill erosion and gullying were mapped.

Evidences of rill-interrill erosion are in general hard to identify from remotely-sensed data (Fig. 2). Moreover, the ephemeral nature of these landforms does not always make their recognition possible. In this study, a preliminary inventory was prepared using orthophotos by mapping all

ACCEPTED MANUSCRIPT

patches with sparse vegetation cover and/or light soil color, which were considered as a signal of rill-interrill erosion processes (Conoscenti et al, 2008). Then, field-checks were carried out to validate the mapped rill-interrill erosion features.

Two different rill geometries were detected: dendritic and parallel patterns. The dendritic pattern rills form a dense branching network that gradually converges downwards (Ludwig et al., 1995). On the contrary, the parallel pattern shows rills that are uniformly distributed on the slope with a relatively close spacing (40 cm), often corresponding to wheel tracks or other tillage consequences. In general, rill-interrill landforms occur on moderately steep cultivated parcels (Fig. 2b,c). The final inventory includes 180 rill-interrill areas with a total extent of 0.83 km^2 (8.75% of the whole catchment).

An existing database of 260 gullies was available for the whole San Giorgio River basin (Conoscenti et al., 2014), whose spatial distribution shows that almost all gullies (98% of total gully length) developed on slopes underlain by clay sediments. Moreover, permanent gullies are often connected to headwater channel networks (Fig. 3a), while ephemeral gullies are mainly controlled by drain outlets of roads, tractor ruts and parcel borders. In addition, some gully head-cuts are located on the depletion zones of shallow landslides, where sediments are poorly consolidated and the concavity of the topography favors concentrated runoff (Conoscenti et. al, 2014). Both V-shaped and U-shaped cross-section profiles for gullies were recognized (Fig. 3b,c); their lateral walls and head-cut sectors are characterized by desiccation cracks, evidence of piping, falls and seepage sub-processes. The morphometric features of the gullies showed a maximum cross section depth of ca. 2 m, while the gully-lengths range from a few meters to around 500 m.

The inventory map prepared is shown in Fig. 4. In order to set the binary status of the dependent variable, the San Giorgio catchment was partitioned into 2 m grid cells. Based on the spatial distribution of rill-interrill and gully landforms, each cell was coded as a positive or negative case depending on the presence or absence of each landform type. The final layer was composed of 189,526 cells coded as positive to rill-interrill erosion, and 49,360 cells coded as positive to gullies.

2.3. Environmental factors

Soil erosion is controlled by numerous factors such as climate, topography, soil properties, vegetation cover and agriculture practices. In the present study, several environmental variables were selected to represent the potential soil erosion controlling factors. In particular, the data set of the predictors consists of four discrete variables (outcropping lithology, land use, slope aspect and landform classification; Table 1) and eight continuous variables (length-slope factor, the

ACCEPTED MANUSCRIPT

topographic wetness index, the stream power index, plan and profile curvatures, elevation, distance to the river and slope angle; Table 2), whose spatial distributions are shown in Fig. 5.

At the basin scale, the soil characteristics are generally described according to the lithology of the parent bedrock (de Vente and Poesen, 2005). Hence, bedrock lithology was used to represent the erodibility of the soils. By integrating an available 1:50,000 geological map of the Imera Settentrionale River basin (Abate et al., 1988), with orthophoto interpretation and field surveys, a 1:10,000 lithological map was derived for the LITHO variable.

Erosion is related to vegetation and land use. A number of papers have demonstrated that the energy of a raindrop's impact is reduced by the presence of a vegetation cover, and that vegetation and organic litter increase surface roughness thus also contrasting water runoff (Cerdan et al., 2002). To explore the effect of vegetation and soil use, a 1:10,000 land use map based on the CORINE land cover classification was derived via orthophoto interpretation.

To model the erosive power of runoff, 10 primary and secondary topographic attributes were included in the statistical analyses. These attributes were derived from a 2-m-cell digital elevation model (DEM), using the System for Automated Geographical Analysis (SAGA) software (Olaya and Conrad, 2008).

Soil erosion susceptibility is influenced by slope aspect (Imeson and Lavee, 1998) in relation to exposure to sunlight and soil aggregate stability. The aspect raster layer extracted from the DEM (Zevenbergen and Thorne, 1987) was classified into eight categorical intervals (Table 1). The topographic wetness index (*TWI*), which is assumed to discriminate between wet and dry areas, was selected to indirectly identify potentially water-saturated zones (Beven and Kirkby, 1979). Because of the importance of the geomorphic characteristics of the drainage basin upstream from gullies and rills (Schumm and Hadley, 1957; Poesen et al., 1996), slope gradient (*SLO*) (Zevenbergen and Thorne, 1987) and upslope drainage area (*SUB*) (Desmet and Govers, 1995) were also used as predictor variables. The relationship between catchment area and slope gradient was described by exploiting two important geomorphological indexes: the stream power index (*SPI*) and the length-slope factor (*LSF*), both modeling runoff and overland flow. *SPI* is a measure of the erosive power of water flow based on the assumption that the discharge is proportional to the specific catchment area and to the slope gradient (Moore et al., 1991; 1993). *LSF* reflects sediment transport capacity, depending on slope steepness and length (Renard et al., 1997). To express the effects of the terrain's local morphometry on the overland flow distribution, plan curvature (*PLC*) and profile curvature (*PRC*) were also included. These attributes depict the spatial distribution of the concavity and convexity of the land surface, which can be associated with flow convergence and divergence, respectively (Moore et al., 1991). The influence of the topographic position was analyzed using the

ACCEPTED MANUSCRIPT

following attributes: elevation (*ELE*), overland flow distance to the river network (*OFD*) and landform classification (*LAND*). The *LAND* raster layer was determined by applying Jenness's (2006) algorithm and classifying the landscape using two topographic positioning index grids at different scales, defined by circular neighborhoods with radii of 100 and 1000 m.

When using stochastic modeling to describe geomorphological phenomena, multicollinearity could be a severe limitation. Some spatial correlations are expected between the predictors, e.g., land-use can be controlled by topography and/or lithology, which in turn directly control the land surface morphology. However, the variable selection by SGT is robust to collinearity amongst predictors and to the presence of irrelevant predictors, and therefore does not require prior variable selection or data reduction (Friedman, 2002; Pittman et al., 2009).

2.4. Modeling strategy and validation procedure

SGT was designed to enhance the prediction accuracy of potentially weak predictors (Hancock et al., 2005), which exploits the Classification And Regression Trees (CART) model (Breiman et al., 1984) as a base predictor in building ensemble machine learning models. It works by a recursive binary stage-wise partitioning process of the input data, which are sequentially broken up into smaller pieces (Berk, 2008). By using SGT, many small classification or regression trees are sequentially built from residual-like measures of the previous tree (Wu et al., 2008).

The purpose of boosting is to apply a forward stage-wise additive modeling and optimize the novel exponential loss function (Freund and Schapire, 1997). At each iteration, a subsample fraction of the training observations is randomly selected (without replacement) to obtain a refined training set that will be used to grow the next tree (Friedman, 2002). In this way, each additional term of the model contributes progressively to refine the overall model accuracy. SGT can be applied to predict both continuous (regression-type model) and discrete (classification-type) response variables, from a set of continuous and/or categorical predictors. It yields a probability value varying from 0 (negative case/absence) to 1 (positive case/presence).

In this study, SGT was applied on balanced (positives/negatives) sampled data sets, each including all the positive (eroded) cells and an equal number of randomly extracted negative (un-eroded) cells. Therefore, samples made of 379,052 and 98,720 cases were obtained, for rill-interrill susceptibility models (RISMs) and gully erosion models (GUSMs), respectively. In addition, four different samples (S1, S2, S3, and S4) were prepared for the RISMs as well as for the GUSMs (S5, S6, S7, and S8) in order to evaluate the robustness of the model building procedure. The four samples of each set share the same positive cases, whilst the subsets of equal number of negative cases were extracted by means of a random sampling without replacement using GIS. In this way,

ACCEPTED MANUSCRIPT

possible sources of variation in the results produced by the particular set of extracted negatives could be detected.

Each sample was first randomly split into calibration (75%) and validation (25%) balanced (positives/negatives) subsets. The calibration subset was then used to fit the SGT model, while the validation subset let us test its prediction skill. The ability of the model in predicting the known (75%) and the unknown (25%) cases was then evaluated, attesting for its goodness of fit and prediction skill, respectively. The comparison of the two types of predictive performance of GUSMs and RISMs also allowed us to evaluate possible overfitting effects. The predictive performance was assessed by constructing receiver operating characteristic (ROC) curves (Goodenough et al., 1974; Lasko et al., 2005) and by computing the values of the area under the ROC curve (*AUC*; Hanley and McNeil, 1982). An ROC curve plots the true positive rate (sensitivity) against the false positive rate (1-specificity), for all possible cut-off values; sensitivity is computed as the fraction of cells hosting erosion features that were correctly classified as susceptible, while specificity is derived from the fraction of cells not-hosting erosion landforms that were correctly classified as non-susceptible. The closer the ROC curve to the upper left corner of the plot (*AUC* = 1), the higher the predictive performance of the model. Following Hosmer and Lemeshow (2000), the prediction skill of the models may be considered acceptable, excellent and outstanding when *AUC* values are higher than 0.7, 0.8 and 0.9, respectively. ROC curves were drawn both for the calibration (training) and validation (test) data sets, in order to verify possible overfitting effects. At the same time, stability through the replicates was employed to estimate the reliability of the model.

However, a complete validation of a susceptibility model, together with an evaluation of its overall *AUC* value, has to be based on the number of prediction successes and failures as well as their spatial distributions. To evaluate this, after RISMs and GUSMs provided the two correspondent soil erosion susceptibility maps, the response variable (the probability of a positive) was binarized into presence or absence by using a threshold probability value. Typically, discrimination between predicted positives and negatives is obtained by setting 0.5 as the probability cut-off (Lucà et al., 2011; Märker et al., 2011; Conoscenti et al., 2013, 2014). However, more objective criteria based on the analysis of the ROC curves have been recently proposed for identifying an optimal threshold value (Fawcett, 2006; Freeman and Moisen, 2008; Gómez Gutiérrez et al., 2009a; Schindler et al., 2011). Freeman et al. (2008) demonstrated that, especially for data sets with very high or very low observed prevalence, accuracy values increase if a threshold criterion is adopted.

ACCEPTED MANUSCRIPT

In the present study, ROC plots were used to determine the optimal cut-off point of the models' score, by adopting Youden's index (*J*) (Youden, 1950), with *J* corresponding to the maximum vertical distance between the ROC curve and the first bisector according to:

$$J = \text{Maximum (sensitivity + specificity} - 1) \quad (1).$$

Finally, in order to evaluate the ability of SGT to construct susceptibility models to soil erosion, the relationships between the predictors and the outcome were analyzed. The tree construction process can be considered as a type of variable selection (Guyon et al., 2006). In particular, SGT provides a relative importance score, which describes the individual contribution of each predictor to the response variable in the tree model. The variables are entered into the model based on their contribution to the impurity reduction at each split (Xie et al., 2009). The relative contribution of the predictor variables to the overall distribution patterns of erosional landforms is based on the improvements of all splits associated with a given variable across all trees in the model (Friedman, 2002). Hence, the variable contribution to the model performance is rescaled across all trees so that the most important variable always gets a score of 100.

In addition, SGT furnishes the partial dependency plots (response curves) of the predictors. A partial dependency plot illustrates the relative index as a function of the predictor in the context of the multivariate model (Cai et al., 2014). The *y*-axis (partial dependence) is a log odds of the presence of erosion landforms. A value of zero corresponds to a zero discrimination (probability of a positive case equals the probability of a negative case). A positive partial dependence indicates preference, while a negative partial dependence indicates avoidance. Together with testing the geomorphological adequacy of the fitted model, exploring the inner structure of a susceptibility model makes it possible to quantitatively define and verify the geomorphological interpretation of a given process from a stochastic perspective.

3. Results

3.1. Performance and reliability of predictive models

The *AUC* values of the RISMs for calibration and validation subsets are reported in Table 3. The validation *AUC* values range from 0.822 to 0.846, indicating an excellent predictive performance for the four data sets. In addition, the *AUC* values for the four data sets are quite similar and the modeling approach can be considered as robust to changes of learning samples. Table 4 shows the *AUC* values obtained for the GUSMs. These models exhibit an excellent to outstanding predictive skill (*AUC* = 0.867 – 0.921) and their performance is quite stable when the learning samples

ACCEPTED MANUSCRIPT

changed. The almost perfect agreement between calibration and validation *AUC* values for both the susceptibility models indicates that no relevant overfitting has been produced.

The best performing RISM and GUSM were used to prepare the maps of susceptibility to rill-interrill erosion (Fig. 6) and gully erosion (Fig. 7) for the entire San Giorgio catchment. By adopting the *J* index, 0.533 and 0.667 probability cut-off values were obtained for the RISM and GUSM susceptibility models, respectively (Fig. 8). Based on these cut-off values, the probability of erosion occurrence for each cell was converted into a binary (positive/negative) prediction to obtain the spatial distribution of cases correctly classified (true positives and negatives) and incorrectly classified (false positives and negatives) for the two susceptibility models. Fig. 9 portrays: i) maps showing the distribution of true positive (*TP*), false positive (*FP*), true negative (*TN*) and false negative (*FN*) cases within the basin, and ii) four-fold plots summarizing the number of the four categories.

Table 5 summarizes the main accuracy statistics obtained for the best models for the whole basin, for both RISM and GUSM. In particular, the RISM susceptibility map correctly explains the presence of 76% of rill-interrill erosion landforms (*TP* or sensitivity) and 77% of un-eroded cases (*TN* or specificity). At the same time, the model provides a prediction in contrast with the geomorphological inventory map (1 − precision) for 76% of the predicted positives (25% for the regressed best data set). The GUSM susceptibility map attests for 76% and 90% of correctly classified positive and negative observed cases (*TP* and *TN*). For the remaining cases, the GUSM map incorrectly predicts 85% of the predicted positives (15% for the regressed best data set).

3.2. Variable importance

Each variable's importance is ranked for both the susceptibility models (Fig. 10). *ELE* and *SPI* are the most important predictors for rill-interrill erosion and gully erosion, respectively. *ASP*, *LAND* and *USE* also showed a strong relationship with rill-interrill erosion. Regarding the occurrence of gullies, *PLC*, *TWI* and *ELE* are the most important predictors after *SPI*.

To better understand the spatial relationships between the erosion landform distribution and the variability of the selected attributes, partial dependence plots were prepared for the three most important predictors of rill-interrill and gully erosion (Fig. 11). Regarding the rill-interrill erosion, a complex trend was obtained for elevation (Fig. 11a), which, however, clearly indicated a positive correlation in the 760–950 m range. East- and southeast-facing slopes are the only aspect conditions that lower the probability of rill-interrill erosion (Fig. 11b), as well as mid-slope ridges and mountain tops (Fig. 11c). *SPI* values greater than approximately 500 m (Fig. 11b), planar

ACCEPTED MANUSCRIPT

concavities (Fig. 11d) and *TWI* values higher than 8 m (Fig. 11f) are the predisposing conditions for gullies.

3.3. Combined susceptibility map

An integrated water erosion susceptibility map for the San Giorgio catchment was prepared (Fig. 12) by heuristically combining the best RISM and GUSM, in which four different cases are discriminated:

(1) If both probability values are lower than their corresponding cut-off values, the pixel is classified as a negative case (not or barely susceptible to soil erosion).

(2) If only the RISM probability value exceeds *J*, then the pixel is mapped as susceptible to rill-interrill erosion.

(3) If only the GUSM probability value exceeds *J*, the pixel is considered as susceptible to gully erosion.

(4) If both probability values are above their *J* values, the pixels are identified as susceptible to rill-interrill erosion and gully erosion simultaneously.

4. Discussion

The results confirmed the use of SGT as suitable for assessing both rill-interrill and gully erosion susceptibilities. In particular, the overall accuracy of the best RISM and GUSM (Fig. 9) were excellent (*AUC* = 0.846) and outstanding (*AUC* = 0.921), respectively. At the same time, the susceptibility maps based on the optimal selection of the cutoff probability values (Table 5), indicate a higher accuracy and specificity for the GUSM. The two models resulted in the same sensitivity (0.76), indicating the same skill in predicting future rill-interrill areas and gullies. However, by looking at the specificity, a larger false positive prediction is produced by the RISM, indicating that the conditions for rill-interrill erosion are more widespread than the current related landforms.

The map shown in Fig. 9a allows us to verify that the false positives are very common in the form of patches throughout the whole basin, with a geometry very similar to the mapped erosion landforms in the same sectors. This suggests that one or more controlling factors, which were not included among the predictors, could be relevant for the activation/inactivation of the rill-interrill erosion in the susceptible areas. We hypothesize that, as these false positive areas are mainly present on arable land, reliable data on the cropping techniques could provide a response to this. At the same time, the general lower accuracy in predicting rill-interrill erosion could be related to the difficulty in recognizing areas affected by this type of erosion. Mapping methods based on the

ACCEPTED MANUSCRIPT

photo-interpretation heavily depend on both the quality of the images and the ephemeral nature of the mapped erosion landforms. Moreover, evidence of rill-interrill erosion is characterized by high temporal variability and can be easily obliterated by tillage operations.

The same analysis for gullies (Fig. 9b) clearly shows that false positives describe very similar spatial patterns to the current gullies (true positives). Very frequently, the false positive patterns define the headward retreatment trend of the current gullies.

The results obtained in this study are compared with those from similar studies, considering differences in the adopted experiment design. Although the use of SGT resulted in excellent prediction, literature discussing SGT for modeling soil erosion is limited. Märker et al. (2011) predicted susceptibility to erosion and mass wasting in the Chianti region (north Italy) using SGT. Their results (*AUC* = 0.931 or 0.981) show outstanding SGT performances. Conoscenti et al. (2014) and Gómez-Gutiérrez et al. (2015) predicted gullies using the same inventory and similar predictors for the San Giorgio River basin by applying logistic regression (LOGREG) and multivariate adaptive regression spline (MARS). Compared to our GUSM results, Conoscenti et al. (2014) obtained a slightly lower accuracy (*AUC* = 0.823) using a 5 m grid-cell model, while Gómez-Gutiérrez et al. (2015) achieved a very similar accuracy (*AUC* = 0.895) for a 4 m grid-cell model, but a lower accuracy (*AUC* = 0.818) for a 2 m grid-cell model.

The findings of the present research can also be compared with a study conducted in southern-central Sicily (Naro River basin, 60 km away from the San Giorgio River) applying conditional analysis (CA) to unique condition units, i.e., homogeneous domains in terms of controlling factors for predicting gully and rill-interrill erosion susceptibility (Conoscenti et al., 2008). Although different metrics were adopted to estimate the overall performance of the predictive models (lift chart: success and prediction-rate curves), the results also confirmed the method's better accuracy in predicting gully erosion than rill-interrill erosion. CA was also used for assessing gully erosion susceptibility in a large basin of southern Sicily (the Magazzolo River basin, 70 km away from the San Giorgio River), obtaining the best *AUC* value of 0.742 (Conoscenti et al., 2013). SGT, together with MARS and LOGREG, resulted in better performances than CA.

Different geo-environmental predictors were selected by the RISM and GUSM (Fig. 10). Topographic indices have the highest contribution in gully erosion prediction, while rill-interrill erosion is mainly influenced by discrete attributes. In particular, elevation, aspect, morphology, land-use and steepness are the most selected variables in the RISMs. Elevation indirectly expresses climate conditions and vegetation distributions on the hillslopes, which are considered as two of the most important factors influencing splash erosion and overland flow. Specifically, the elevation response curve (Fig. 11a) shows a positive correlation with probability of rill-interrill erosion if the

ACCEPTED MANUSCRIPT

altitude is between 760 and 950 m a.s.l. This result may be explained by interpreting elevation as a proxy for rainfall intensity and considering that an elevation higher than 950 m a.s.l. only occurs in the extreme northern sector of the basin, where other factors, such as a high slope gradient and hard bedrock, are unfavorable for rill-interrill erosion.

Another important predictor for rill-interrill erosion is slope aspect (Fig. 11c), which affects solar insolation, evapotranspiration, flora and fauna distribution and abundance (Wilson and Gallant, 2000). In particular, for rill-interrill erosion, north-facing slopes are the most favorable. This result seems to be in conflict with previous studies (e.g. Marque's and More, 1992; Calvo-Cases et al., 2003; López-Vicente et al., 2011), which indicate that south-facing slopes are more eroded because less soil moisture leads to less vegetation growth and consequentially less protection. However, more than 90% of the study area is cultivated; consequently, the effect of vegetation protection is negligible (Fig. 5).

The results also show that rill-interrill erosion is active in upland zones, mid-slope drainages, plain zones and the upper portion of hill landform classes (Fig. 11e). Upland zones and the upper portions of slopes are characterized by convex surfaces. In these portions, soils are thin and poorly developed, overlying highly weathered bedrock where soil removal mainly occurs by raindrop impact and shallow surface flow. The increased steepness in the mid-slope accelerates rill development.

This study has quantified the role of land-use and slope steepness in the rill-interrill erosion model (Fig. 10). The gentle slope surfaces of the San Giorgio River basin are largely devoted to cereals whose cropping cycle leaves the soil unprotected during the rainfall season between October and February. Therefore, the total runoff from cereal fields is often directly correlated to the annual precipitation (García-Ruiz, 2010). On the contrary, pastures located on the steeper sectors of the basin are dominated by shrubs. The shrubs protect the soil, improving organic matter content, soil structure and water infiltration (Koulouri and Giourga, 2007).

Regarding gully erosion, *SPI*, *PLC* and *TWI* are the most influential independent variables (Fig. 10). The response curves for gully erosion show that *SPI* values larger than 100 m are positively correlated with gullying (fig. 11b), while *TWI* values larger than 7.6 m have a positive influence on GUSM construction (fig. 11f). Several researchers have used *TWI* and *SPI* to predict ephemeral gullies and identify their threshold values for gully initiation (Thorne et al., 1986; Moore et al., 1988; Montgomery and Dietrich, 1994). Moreover, the *PLC* response curve (Fig. 11d) shows a maximum contribution of concave zones (*PLC* negative values) on the study area for gullying. These results provide further information about topographic thresholds for gully initiation and development in the landscape.

ACCEPTED MANUSCRIPT

The variables important for the GUSM are similar to those of previous studies for the same study area but with different statistical approaches. Conoscenti et al. (2014) identified *PLC*, *SPI*, *PRC* and *TWI* as the most significant topographic predictors for gully erosion, while Gomez Gutierrez et al. (2015) identified *TWI* and *ELE* as the most important.

By integrating the results of rill-interrill erosion and gully erosion modeling, a combined map of erosion susceptibility was produced (Fig. 12). This map shows ordinal categories of susceptibility to water erosion rather than explicit probability of occurrence. Few previous studies have explored susceptibility models that predict the location of different erosion processes in the same area. Marker et al. (2011) created a map where five erosion classes were represented: no erosion, rill-interrill erosion; severe rill-interrill and gully erosion; inactive landslides; and active landslides. Giessen et al. (2007) constructed a model to predict superficial erosion processes (gullies, rills, and mass movements) and subterranean processes (sinkholes and tunnels). Although these studies included erosion models with more than one response variables, they do not establish an optimal cut-off value for discriminating between the two categories of response variable. On the contrary, the present paper tested the possibility of optimizing a threshold value for zoning soil erosion susceptibility.

In the San Giorgio River basin, pixels identified as susceptible to severe soil erosion (prone to rill-interrill erosion and gully erosion) represent only 2% of the whole catchment, and are concentrated in the highly steep north-facing slopes. Areas classified exclusively as "susceptible to rill-interrill erosion" are distributed as patches over a large part of the basin (26%), mainly located on smooth slopes above the drainage lines or on the upland areas. Zones prone to gullying are concentrated in valley bottoms of zero order catchments and in concave slopes (10%). Finally, surfaces classified as having low or extremely low susceptibility to water erosion correspond to more than 62% of the basin. These zones are mainly located on the upper and mid-slope portions of hills, characterized by low gradient and convex slopes. These results show that, although the two erosion phenomena are strictly connected and often coupled in nature, the combined erosion susceptibility map makes it possible to identify the specific conditions that favor rill-interrill erosion and gully erosion, and to discriminate between the two.

5. Conclusions

The present study carried out in the San Giorgio River catchment proved that SGT is a useful and reproducible method to generate erosion susceptibility models. It showed a high and stable accuracy in evaluating soil susceptibility to rill-interrill and gully erosion. Moreover, the use of a statistical approach permitted us to objectively measure the contribution of each predictor in explaining the

ACCEPTED MANUSCRIPT

response variable of the model. A different suite of important predictors was selected for the two erosion models. *ELE*, *ASP*, *LAND* and *USE* were the most important variables in rill-interrill erosion modeling, while *SPI*, *PLC* and *TWI* were the most important variables for predicting gullying. Because the studied catchment is representative of the cultivated Mediterranean Apennine areas, the obtained results may be applied to wider areas. A combined map representing the spatial distribution of water erosion susceptibility over the basin was produced. It is useful for local administrators to identify the most susceptible areas to erosion within their jurisdiction and to develop effective soil conservation strategies.

Acknowledgments
This research was developed in the framework of the projects: FLUMEN (project number: 318969), funded by the EU (call identifier: FP7-PEOPLE-2012-IRSES). We thank the editor Prof. Takashi Oguchi and the two anonymous reviewers for their suggestions and comments. We also wish to express our gratitude to Cassandra Funsten (USA) for her help with the linguistic revision.

References

Abate, B., Renda, P., Tramutoli, M., 1988. Carta Geologica dei Monti di Termini Imerese e delle Madonie occidentali (Sicilia Centro-settentrionale). Dipartimento di Geologia e Geodesia dell'Università di Palermo, STableTip, Salomone. Roma.

Auzet, A.V., Boiffin, J., Ludwig, B., 1995. Concentrated flow erosion in cultivated catchments: influence of soil surface state. Earth Surface Processes and Landforms 20, 759-767. doi:10.1002/esp.3290200807.

Ballabio, C., Sterlacchini, S., 2012. Support Vector Machines for Landslide Susceptibility Mapping: The Staffora River Basin Case Study, Italy. Mathematical Geosciences 44, 47-70. doi:10.1007/s11004-011-9379-9.

Berk, R.A., 2008. Statistical Learning from a Regression Perspective. New York. Springer, pp. 360. ISBN: 978-0-387-77500-5.

Beven K.J., Kirkby M.J., 1979. A physically based, variable contributing area model of basin hydrology. Hydrologic Sciences Bulletin 24, 43-69. doi:10.1080/02626667909491834.

Bocco, G., 1991. Gully erosion: processes and models. Progress in Physical Geography 15 (4), 392-406. doi:10.1177/030913339101500403.

Brenning, A., 2005. Spatial prediction models for landslide hazards: review, comparison and evaluation. Natural Hazards and Earth System Sciences (5), 853–862.

ACCEPTED MANUSCRIPT

Breiman, L., Friedman, J.H., Olshen, R.A., Stone, C.J., 1984. Classification and Regression Trees. Wadsworth International Group, Belmont, California, USA. Taylor & Francis pp 368. ISBN: 978-0-412-04841-8.

Bryan, R.B., 1990. Knickpoint evolution in rillwash. Catena Supplement 17, 111–132.

Bryan, R.B., 2000. Soil erodibility and processes of water erosion on hillslope. Geomorphology 32(3-4), 385–415. doi:10.1016/S0169-555X(99)00105-1.

Bryan, R.B., Kuhn, N.J., 2002. Hydraulic conditions in experimental rill confluences and scour in erodible soils. Water Resources Research, 38 (5). doi:10.1029/2000WR000140.

Calvo-Cases, A., Boix-Fayos, C., Imeson, A., 2003. Runoff generation, sediment movement and soil water behaviour on calcareous (limestone) slopes of some Mediterranean environments in southeast Spain. Geomorphology 50, 269–291. doi:10.1016/S0169-555X(02)00218-0

Cai, T., Huettmann, F., Guo, Y., 2014. Using Stochastic Gradient Boosting to Infer Stopover Habitat Selection and Distribution of Hooded Cranes Grus *monacha* during Spring Migration in Lindian, Northeast China. PLoS ONE 9(2): e89913. doi:10.1371/journal.pone.0089913.

Carrara, A., Pike, R.J., 2008. GIS technology and models for assessing landslide hazard and risk. Geomorphology 94(3–4), 257-260. doi:10.1016/j.geomorph.2006.07.042.

Cerdan, O., Le Bissonnais, Y., Souchère, V., Martin, P., Lecomete, V., 2002. Sediment concentration in interrill flow: interactions between soil surface conditions, vegetation and rainfall. Earth Surface Processes and Landforms 27(2), 193-205. doi:10.1002/esp.314.

Chaplot, V.A.M., Le Bissonnais, Y., 2003. Runoff features for interrill erosion at different rainfall intensities, slope lengths, and gradients in an agricultural loessial hillslope. Soil Science Society of America Journal, 67(3), 844-851. doi:10.2136/sssaj2003.8440.

Chaplot, V., Giboire, G., Marchand, P., Valentin, C., 2005. Dynamic modelling for linear erosion initiation and development under climate and land-use changes in northern Laos. Catena, 63(2-3), 318-328. doi:10.1016/j.catena.2005.06.008.

Conforti, M., Aucelli, P.P.C., Robustelli, G., Scarciglia, F., 2010. Geomorphology and GIS analysis for mapping gully erosion susceptibility in the Turbolo stream catchment (Northern Calabria, Italy). Natural Hazards 56(3), 881–898. doi:10.1007/s11069-010-9598-2.

Conoscenti, C., Di Maggio, C., Rotigliano, E., 2008. Soil erosion susceptibility assessment and validation using a geostatistical multivariate approach: a test in Southern Sicily. Natural Hazards 46, 287–305. doi:10.1007/s11069-007-9188-0.

Conoscenti, C., Agnesi, V., Angileri, S.E., Cappadonia, C., Rotigliano, E., Märker, M., 2013. A GIS-based approach for gully erosion susceptibility modelling: a test in Sicily, Italy. Environmental Earth Sciences 70, 1179–1195. doi:10.1007/s12665-012-2205-y.

Conoscenti, C., Angileri, S.E., Cappadonia, C., Rotigliano, E., Agnesi, V., Märker, M., 2014. Gully erosion susceptibility assessment by means of GIS-based logistic regression: a case of Sicily (Italy). Geomorphology 204, 399–411. doi:10.1016/j.geomorph.2013.08.021.

ACCEPTED MANUSCRIPT

Conoscenti, C., Ciaccio, M., Caraballo-Arias, N.A., Gómez-Gutiérrez, Á., Rotigliano, E., Agnesi, V., 2015. Assessment of susceptibility to earth-flow landslide using logistic regression and multivariate adaptive regression splines: A case of the Belice River basin (western Sicily, Italy) Geomorphology 242, 49–64. doi:10.1016/j.geomorph.2014.09.020.

Costanzo, D., Cappadonia, C., Conoscenti, C., Rotigliano, E., 2012. Exporting a Google EarthTM aided earth-flow susceptibility model: a test in central Sicily. Natural Hazards 61(1), 103–114. doi:10.1007/s11069-011-9870-0.

Costanzo, D., Chacòn, J., Conoscenti, C., Irigaray, C., Rotigliano, E., 2013. Forward logistic regression for earth-flow landslide susceptibility assessment in the Platani River basin (Southern Sicily, Italy). Landslides 11, 639–653. doi:10.1007/s10346-013-0415-3.

de Vente, J., Poesen, J., 2005. Predicting soil erosion and sediment yield at the basin scale: Scale issues and semi-quantitative models. Earth-Science Reviews 71(1-2), 95-125. doi:10.1016/j.earscirev.2005.02.002.

Desmet, P.J.J., Govers, G., 1995. GIS-based simulation of erosion and deposition patterns in an agricultural landscape: a comparison of model results with soil map information. Catena 25(1-4), 389-401. doi:10.1016/0341-8162(95)00019-O.

Desmet, P.J.J., Govers, G., 1997. Two-dimensional modelling of the within-field variation in rill and gully geometry and location related to topography. Catena 29 (3-4), 283-306. doi:10.1016/S0341-8162(96)00074-4.

Di Stefano, C., Ferro, V., Pampalone, V., Sanzone, F., 2013. Field investigation of rill and ephemeral gully erosion in the Sparacia experimental area, South Italy. Catena 101, 226-234. doi:10.1016/j.catena.2012.10.012.

Dunne, T., Aubry, B.F., 1986. Evaluation of Horton's theory of sheet wash and rill erosion on the basis of field experiments. In: Abrahams, A.D. (Ed.), Hillslope Processes. Allen and Unwin, Boston, pp. 31–53.

Elith, J., Leathwick, J.R., Hastie, T., 2008. A working guide to boosted regression trees. Journal of Animal Ecology 77(4), 802-813. doi:10.1111/j.1365-2656.2008.01390.x.

Emmett, W.W., 1970. The hydraulics of overland flow on hillslopes. U.S. Geological Survey. Professional Paper 666-2A, pp 68.

Fawcett, T., 2006. An introduction to ROC analysis. Pattern Recognition Letters, 27 (8) 861–874. doi:10.1016/j.patrec.2005.10.010.

Fierotti, G., Dazzi, C., Raimondi, S., 1988. Carta dei Suoli della Sicilia 1:25,000. Regione Siciliana, Assessorato Territorio e Ambiente, Università degli Studi di Palermo, Facoltà di Agraria, Istituto di Agronomia Generale, Palermo (Italy).

Flügel, W.A., Märker, M., Moretti, S., Rodolfi, G., Sidorchuk, A., 2003. Integrating geographical information systems, remote sensing, ground truthing and modelling approaches for regional erosion classification of semi-arid catchments in South Africa. Hydrological Processes 17 (5), 929-942. doi: 10.1002/hyp.1171.

ACCEPTED MANUSCRIPT

Foster, G.R., 1986. Understanding ephemeral gully erosion. Soil Conservation, vol. 2. National Academy of Science Press, Washington, DC, pp. 90-125.

Freeman, E.A., Moisen, G.G., 2008. A comparison of the performance of threshold criteria for binary classification in terms of predicted prevalence and kappa. Ecological Modelling 217(1-2), 48-58. doi:10.1016/j.ecolmodel.2008.05.015.

Freund, Y., Schapire, R.E., 1997. A decision-theoretic generalization of on-line learning and an application to boosting. Journal of Computer and System Sciences 55(1), 119–139. doi:10.1006/jcss.1997.1504.

Friedman, J.H., 1999. Stochastic gradient boosting. Technical Report. Department of Statistics, Stanford University.

Friedman, J.H., 2001. Greedy function approximation: A gradient boosting machine. The Annals of Statistics 29(5), 1189-1232. doi:10.1214/aos/1013203451

Friedman, J.H., 2002. Stochastic gradient boosting. Computational Statistics and Data Analysis 38(4), 367-378. doi:10.1016/S0167-9473(01)00065-2.

García-Ruiz, J.M., 2010. The effects of land uses on soil erosion in Spain: A review. Catena 81(1), 1-11. doi:10.1016/j.catena.2010.01.001.

Geissen, V., Kampichler, C., López-de Llergo-Juárez, J.J., Galindo-Acántara, A., 2007. Superficial and subterranean soil erosion in Tabasco, tropical Mexico: Development of a decision tree modeling approach. Geoderma 139(3-4), 277–287. doi:10.1016/j.geoderma.2007.01.002.

Giménez, R., Govers, G., 2001. Interaction between bed roughness and flow hydraulics in eroding rills. Water Resources Research 37(3), 791–799. doi:10.1029/2000WR900252.

Gómez Gutiérrez, Á., Schnabel, S., Lavado Contador, J.F., 2009a. Using and comparing two nonparametric methods (CART and MARS) to model the potential distribution of gullies. Ecological Modelling 220(24), 3630-3637. doi:10.1016/j.ecolmodel.2009.06.020.

Gómez Gutiérrez, Á., Schnabel, S., Felicísimo, Á.M., 2009b. Modelling the occurrence of gullies in rangelands of southwest Spain. Earth Surface Processes and Landforms 34(14), 1894–1902. doi:10.1002/esp1881.

Gómez Gutiérrez, Á., Conoscenti, C., Angileri, S.E., Rotigliano, E., Schnabel, S., 2015. Using Topographical attributes to model the spatial distribution of gullying from two Mediterranean basins: advantages and limitations. Natural Hazards. doi:10.1007/s11069-015-1703-0.

Goodenough, D.J., Rossmann, K., Lusted, L.B., 1974. Radiographic applications of Receiver Operating Characteristic (ROC) curves. Radiology 110(1), 89-95. doi: 10.1148/110.1.89.

Govers, G., 1985. Selectivity and transport capacity of thin flows in relation to rill erosion. Catena 12(1), 35-49. doi:10.1016/S0341-8162(85)80003-5.

Govers, G., Rauws, G., 1986. Transporting capacity of overland flow on plane and on irregular beds. Earth Surface Processes and Landforms 11(5), 515-524. doi:10.1002/esp.3290110506.

ACCEPTED MANUSCRIPT

Govers, G., Giménez, R.; Van Oost, K., 2007. Rill erosion: Exploring the relationship between experiments, modelling and field observations. Earth-Science Reviews 84 (3-4), 87-102. doi:10.1016/j.earscirev.2007.06.001.

Guyon, I., Nikravesh, M., Gunn, S., Zadeh, L.A., 2006. Feature Extraction. Foundations and applications. Studies in Fuzziness and Soft Computing. Guyon, I., Nikravesh, M., Gunn, S., Zadeh, L.A., (Eds.). Springer-Verlag Berlin Heidelberg, pp. 778. doi:10.1007/978-3-540-35488-8.

Guzzetti, F, Carrara, A, Cardinali, M, Reichenbach, P., 1999. Landslide hazard evaluation: a review of current techniques and their application in a multi-scale study, Central Italy. Geomorphology 31(1–4), 181–216. doi:10.1016/S0169-555X(99)00078-1.

Guzzetti, F., Reichenbach, P., Ardizzone, F., Cardinali, M., Galli, M., 2006. Estimating the quality of landslide susceptibility models. Geomorphology 81 (1–2), 166-184. doi:10.1016/j.geomorph.2006.04.007.

Hancock, T., Put, R., Coomans, D., Vander Heyden, Y., Everingham, Y., 2005. A performance comparison of modern statistical techniques for molecular descriptor selection and retention prediction in chromatographic QSRR studies. Chemometrics and Intelligent Laboratory Systems 76 (2), 185-196. doi:10.1016/j.chemolab.2004.11.001.

Hanley, J.A., McNeil, B.J., 1982. The meaning and use of the area under a receiver operating characteristic (ROC) curve. Radiology 143(1), 29-36. doi: 10.1148/radiology.143.1.7063747.

Hosmer, D.W., Lemeshow, S., 2000. Applied logistic regression. In: John Wiley & Sons (2nd Eds.), New York, pp.160-166. doi:10.1002/0471722146.

Imeson, A.C., Kwaad, F.J.P.M., 1980. Gully types and gully prediction. Geografisch Tijdschrift 14, pp. 430-441.

Imeson, A.C., Lavee, H., 1998. Soil Erosion and Climate Change: The Transect Approach and the Influence of Scale. Geomorphology 23(2–4), 219–227. doi:10.1016/s0169-555x(98)00005-1.

Imeson, A.C., Kwaad, F.J.P.M., Mücher, H.J., 1980. Hillslope processes and deposits in forested areas of Luxembourg. In: Cullingford R.A., Davidson D.A. and Lewin J. (Eds), Timescales in Geomorphology, Wiley, New Youk, pp. 31-42.

Jenness, J., 2006. Topographic Position Index. Extension for ArcView 3.x, v. 1.2. Jenness Enterprises. http://www.jennessent.com/arcview/tpi.htm.

Kosmas, C., Danalatos, N., Cammeraat, L.H., Chabart, M., Diamantopoulos, J., Farand, R., Gutierrez, L., Jacob, A., Marques, H., Martinez-Fernandez, J., Mizara, A., Moustakas, N., Nicolau, J.M., Oliveros, C., Pinna, G., Puddu, R., Puigdefabregas, J., Roxo, M., Simao, A., Stamou, G., Tomasi, N., Usai D., Vacca, A., 1997. The effect of land use on runoff and soil erosion rate under Mediterranean conditions. Catena 29, 45 -59. doi:10.1016/S0341-8162(96)00062-8.

Koulouri, M., Giourga, C., 2007. Land abandonment and slope gradient as key factors of soil erosion in Mediterranean terraced lands. Catena 69(3), 274-281. doi:10.1016/j.catena.2006.07.001.

ACCEPTED MANUSCRIPT

Lal, R., 2003. Offsetting global CO2 emissions by restoration of degraded soils and intensification of world agriculture and forestry. Land Degradation & Development, vol. 14(3), 309-322. doi:10.1002/ldr.562.

Lasko, T.A., Bhagwat, J.G., Zou, K.H., Ohno-Machado, L., 2005. The use of receiver operating characteristic curves in biomedical informatics. Journal of biomedical informatics 38(5), 404-415. doi:10.1016/j.jbi.2005.02.008.

Lombardo, L., Cama, M., Märker, M., Rotigliano, E., 2014. A test of transferability for landslides susceptibility models under extreme climatic events: application to the Messina 2009 disaster. Natural Hazards 74(3), 1951-1989. doi:10.1007/s11069-014-1285-2.

Lombardo, L., Cama, M., Conoscenti, C., Märker, M., Rotigliano, E., 2015. Binary logistic regression versus stochastic gradient boosted decision trees in assessing landslide susceptibility for multiple-occurring landslide events: application to the 2009 storm event in Messina (Sicily, southern Italy). Natural Hazards. doi:10.1007/s11069-015-1915-3.

López-Vicente, M., Lana-Renaul, N., García-Ruiz, J.M., Navas, A., 2011. Assessing the potential effect of different land cover management practices on sediment yield from an abandoned farmland catchment in the Spanish Pyrenees. Journal of Soils and Sediments 11, 1440–1455. doi:10.1007/s11368-011-0428-2.

Lucà, F., Conforti, M., Robustelli, G., 2011. Comparison of GIS-based gullying susceptibility mapping using bivariate and multivariate statistics: Northern Calabria, South Italy. Geomorphology 134(3-4), 297-308. doi:10.1016/j.geomorph.2011.07.006.

Ludwig, B., Boiffin, J., Chadluf, J., Auzet, A.V., 1995. Hydrological structure and erosion damage caused by concentrated flow in cultivated catchments. Catena 25(1-4), 227-252. doi:10.1016/0341-8162(95)00012-H.

Magliulo, P., 2010. Soil erosion susceptibility maps of the Janare Torrent Basin (Southern Italy). Journal of Maps 6(1), 435-447. doi:10.4113/jom.2010.1116.

Magliulo, P., 2012. Assessing the susceptibility to water-induced soil erosion using a geomorphological, bivariate statistics-based approach. Environmental Earth Sciences 67(6), 1801–1820. doi:10.1007/s12665-012-1634-y.

Marjanović, M., Kovačević, M., Bajat, B., Voženílek, V., 2011. Landslide susceptibility assessment using SVM machine learning algorithm. Engineering Geology 123(3), 225-234. doi:10.1016/j.enggeo.2011.09.006.

Marque´s, M.A., Mora, E., 1992. The influence of aspect on runoff and soil loss in a Mediterranean burnt forest (Spain). Catena 19, 333–344. doi:10.1016/0341-8162(92)90007-X.

Märker, M., Pelacani, S., Schröder, B., 2011. A functional entity approach to predict soil erosion processes in a small Plio-Pleistocene Mediterranean catchment in Northern Chianti, Italy. Geomorphology 125(4), 530-540. doi:10.1016/j.geomorph.2010.10.022.

Merkel, W.H., Woodward, D.E., Clarke, C.D., 1988. Ephemeral gully erosion model (EGEM). Modelling Agricultural, Forest, and Rangeland Hydrology. American Society of Agricultural Engineers Publication 7, 315-323.

ACCEPTED MANUSCRIPT

Merritt, E., 1984. The identification of four stages during micro-rill development. Earth Surface Processes and Landforms 9 (5), 493-496. doi:10.1002/esp.3290090510.

Montana, G., Polito, A.M., Caruso, A., Azzaro, E., 2011. Le "argille ceramiche" della Sicilia occidentale e centrale. In: IlionBooks (Eds.), Enna, pp. 21. ISBN 978-88-903626-2-0.

Montgomery, D.R., Dietrich, W.E., 1988. Where do channels begin?. Nature 336, 232-234. doi: 10.1038/336232a0.

Montgomery, D.R., Dietrich, W.E., 1994. Landscape dissection and drainage area-slope thresholds. In: Kirkby, M.J. (Ed.), Process Models and Theoretical Geomorphology. Wiley, Chichester, UK, pp. 221-246.

Moore, I.D., Burch, G.J., 1986. Physical Basis of the Length-slope Factor in the Universal Soil Loss Equation. Soil Science Society of America Journal 50(5), 1294-1298. doi:10.2136/sssaj1986.03615995005000050042x.

Moore, I.D., Burch, G.J., Mackenzie, D.H., 1988. Topographic effects on the distribution of surface soil water and the location of ephemeral gullies. Transactions of the ASAE 31(4), 1098-1107. doi:10.13031/2013.30829.

Moore, I.D., Grayson, R.B., Ladson, A.R., 1991. Digital terrain modeling: a review of hydrological geomorphological and biological applications. Hydrological Processes 5(3), 3-30. doi:10.1002/hyp.3360050103.

Moore, I.D., Gessler, P.E., Nielsen, G.A., Peterson, G.A., 1993. Soil attribute prediction using terrain analysis. Soil Science Society of America Journal 57(2), 443-452. doi:10.2136/sssaj1993.03615995005700020026x.

Neuhäuser, B., Terhorst, B, 2007. Landslide susceptibility assessment using ''weights-of-evidence'' applied to a study area at the Jurassic escarpment (SW-Germany). Geomorphology 86(1-2), 12-24. doi:10.1016/j.geomorph.2006.08.002.

Olaya, V., Conrad, O., 2008. Geomorphometry in SAGA. In: Hengl, T., Reuter, H.I. (Eds.), Geomorphometry: Concepts, Software, Applications. Developments in Soil Science 33, Elsevier, pp. 293-308.

Patton, P.C., Schumm, S.A., 1975. Gully erosion, Northwestern Colorado: A threshold phenomenon. Geology 3(2), 88-90. doi:10.1130/0091-7613(1975)3<88:GENCAT>2.0.CO;2.

Pittman, S.J., Costa, B.M., Battista, T.A., 2009. Using Lidar Bathymetry and Boosted Regression Trees to Predict the Diversity and Abundance of Fish and Corals. Journal of Coastal Research, 10053, 27–38. doi: 10.2112/SI53-004.1

Poesen, J.W., Vandaele, K., Van Wesemael, B., 1996. Contribution of gully erosion to sediment production on cultivated lands and rangelands. Proceedings of the Exeter Symposium, Erosion and Sediment Yield: Global and Regionala Perspeecttives. IAHS Publications 236, pp. 251-266. ISBN: 094-7571-89-2.

Poesen, J.W., Vandekerckhove, L., Nachtergaele, J., Oostwoud Wijdenes, D., Vestraeten, G. and van Wesemael, B., 2002. Gully erosion in dryland environments. In: Bull, L.J., and Kirkby, M.J.,

ACCEPTED MANUSCRIPT

(Eds.), Dryland rivers: Hydrology and Geomorphology of Semi-arid Channels. John Wiley and Sons, Cichester. pp. 229-262.

Poesen, J.W., Nachtergaele, J., Verstraeten, G., Valentin, C., 2003. Gully erosion and environmental change: importance and research needs. Catena 50(2-4), 91-133. doi:10.1016/S0341-8162(02)00143-1.

Poesen, J.W., Vanwalleghem, T., de Vente, J., Knapen, A., Verstraeten, G. and Martínez-Casasnovas, J.A., 2006. Gully Erosion in Europe. In: Boardman J. and Poesen J.W. (Eds.), Soil Erosion in Europe. John Wiley & Sons, Ltd, Chichester, UK. doi:10.1002/0470859202.ch39.

Pozdnoukhov, A., Matasci, G., Kanevski, M., Purves, R.S., 2011. Spatio-temporal avalanche forecasting with support vector machines. Natural Hazards and Earth System Sciences 11, 367-382. doi:10.5194/nhess-11-367-2011.

Prosser, I.P, Dietrich, W.E., Stevenson, J., 1995. Flow resistance and sediment transport by concentrated overland flow in a grassland valley. Geomorphology 13(1-4), 71-86. doi:10.1016/0169-555X(95)00020-6.

Renard, K.G., Foster, G.R., Weesies, G.A., McCool, D.K., Yoder, D.C., 1997. Predicting Soil Erosion by Water: a Guide to Conservation Planning with the Revised Universal Soil Loss Equation (RUSLE). In: Predicting rainfall erosion losses: a guide to conservation planning. Agricultural Handbook 703. US Department of Agriculture, Washington, DC.

Rose, C.W., 1985. Developments in soil erosion and deposition models. In: Stewart, B.A. (Eds.), Advances in soil science, vol. 2. Springer-Verlag, New York, pp. 1-63. doi:10.1007/978-1-4612-5088-3_1.

Rossi, M., Guzzetti, F., Reichenbach, P., Mondini, A.C., Peruccacci, S., 2010. Optimal landslide susceptibility zonation based on multiple forecasts. Geomorphology 114(3), 129-142. doi:10.1016/j.geomorph.2009.06.020.

Rotigliano, E., Cappadonia, C., Conoscenti, C., Costanzo, D., Agnesi, V., 2011. Slope units-based flow susceptibility model: using validation tests to select controlling factors. Natural Hazards 58(3), 981-999. doi:10.1007/s11069-010-9708-1.

Sidorchuk, A., 1999. Dynamic and static models of gully erosion. Catena 37(3-4), 401-414. doi:10.1016/S0341-8162(99)00029-6.

Schindler, D., Grebhan, K., Albrecht ,A., Schönborn, J., Kohnl, U., 2011. GIS-based estimation of the winter storm damage probability in forests: a case study from Baden-Wuerttemberg (Southwest Germany). International Journal of Biometeorology 56(1), 57-69. doi:10.1007/s00484-010-0397-y.

Schumm, S.A., Hadley, R.F., 1957. Arroyos and the semiarid cycle of erosion: American Journal of Science 255(3), 161-174. doi:10.2475/ajs.255.3.161.

Thorne, C.R., Zevenbergen, L.W., Grissinger, F.H., Murphey, J.B., 1986. Ephemeral gullies as sources of sediment. In: Proceedings of the Fourth Federal Interagency Sedimentation Conference, Las Vegas, 3152-3161.

ACCEPTED MANUSCRIPT

Torri, D., Sfalanga, M., Chisci, G., 1987. Threshold conditions for incipient rilling. Catena Supplement 8, 97-105.

Valentin, C., Poesen, J., Li, Y., 2005. Gully erosion: Impacts, factors and control. Catena 63 (2-3), 132-153. doi:10.1016/j.catena.2005.06.001.

Vandekerckhove, L., Poesen, J., Oostwoud Wijdenes, D., de Figueiredo, T., 1998. Topographical thresholds for ephemeral gully initiation in intensively cultivated areas of the Mediterranean. Catena 33 (3-4), 271-292. doi:10.1016/S0341-8162(98)00068-X.

Vergari, F., Della Seta M., Del Monte M., Fredi P., Lupia Palmieri E., 2011. Landslide susceptibility assessment in the Upper Orcia Valley (Southern Tuscany, Italy) through conditional analysis: a contribution to the unbiased selection of causal factors. Natural Hazards and Earth System Science 11(5), 1475-1497. doi: 10.5194/nhess-11-1475-2011.

Wilson, J.P., Gallant J.C. , 2000 Terrain Analysis: Principles and Applications. In: John Wiley & Sons Ltd. (Eds.), New York, USA.

Wirtz, S., Seeger, M., Ries, J.B., 2012. Field experiments for understanding and quantification of rill erosion processes. Catena, 91, 21-34. doi:10.1016/j.catena.2010.12.002.

Wu, X., Kumar, V., Ross Quinlan, J., Ghosh, J., Yang, Q., Motoda, H., McLachlan, G.J., Ng, A., Liu, B., Yu, P.S., Zhou, Z.-H., Steinbach, M., Hand, D.J., Steinberg, D., 2008. Top 10 algorithms in data mining. Knowledge and Information Systems 14(1), 1–37. doi:10.1007/s10115-007-0114-2.

Xie, J., Rojkova, V., Pal, S., Coggeshall, S., 2009. A combination of boosting and bagging for KDD Cup 2009 - Fast scoring on a large database. Journal of Machine Learning Research, Workshop and Conference Proceedings 7, 35–43.

Yao, C., Lei, T., Elliot, W. J., McColl, D.K., Zhao, J., Chen, S., 2008. Critical conditions for rill initiation. Transactions of the ASABE, 51(1), 107-114. doi:0001-2351. 10.13031/2013.24231.

Youden, W.J, 1950. Index for rating diagnostic tests. Cancer 3(1), 32-35. doi:10.1002/1097-0142(1950)3:1<32::AID-CNCR2820030106>3.0.CO;2-3

Zevenbergen, L.W., Thorne, C.R., 1987. Quantitative analysis of land surface topography. Earth Surface Processes and Landforms 12(1), 47-56. doi:10.1002/esp.3290120107.

Figure Captions

Fig. 1. Study area. (a) Location in Sicily. (b) Imera Meridionale River basin. (c) Orthophotos (year 2007) of the San Giorgio River catchment.

ACCEPTED MANUSCRIPT

Fig. 2. Examples of rill-interrill erosion on cultivated soils in the San Giorgio River basin. (a) Area affected by rill-interrill erosion processes. (b) Development of a single rill. (c) Numerous closely spaced rills.

Fig. 3. Examples of gullies within the San Giorgio River basin. (a) Permanent gully connected to its headwater channel network. (b) V-shaped gully. (c) U-shaped gulley.

Fig. 4. Spatial distribution of water erosion landforms in the San Giorgio River basin.

Fig. 5. Maps of the selected environmental controlling factors.

Fig. 6. Rill-interrill erosion susceptibility maps. (a) Whole basin. (b) Zoomed sector of the basin with landforms.

Fig. 7. Gully erosion susceptibility maps. (a) Whole basin. (b) Zoomed sector.

Fig. 8. ROC-plots for the rill-interrill erosion susceptibility model (RISM) and the gully erosion susceptibility model (GUSM). The red segment corresponds to the maximum Youden index (*J*) on the ROC-curve.

Fig. 9. RISM (a) and GUSM (b) regionalized maps showing the spatial distribution of true positive (*TP*), false positive (*FP*), true negative (*TN*), and false negative (*FN*) cases. In the lower left corner, the relative four-fold plots are presented.

Fig. 10. Relative importance of variables (%), scaled in relation to the most important predictor (elevation, *ELE*, and the stream power index, *SPI*, for rill-interrill and gully erosion, respectively). *PLC*: plan curvature, *TWI*: topographic wetness index, *ASP*: aspect, *OFD*: overland flow distance, *LITHO*: lithology, *LAND*: landform, *USE*: land use, *PRC*: profile curvature, *SLO*: slope angle, *LSF*: length-slope factor.

Fig. 11. Partial dependence plots of the three most important predictors for rill-interrill erosion and gully erosion. Values on the *x*-axis represent the response variable and the *y*-axis represents a relative index of occurrence.

Fig. 12. Combined water erosion susceptibility map for the San Giorgio River basin.

Table Captions

Table 1. Discrete variables included in the erosion models. Their codes and the percentage of the surface covered by each variable are shown.

Table 2. Continuous variables included in the erosion models. Their codes, SI units, mean values and standard deviation values are shown.

Table 3. Area under the receiver operating characteristic curve (*AUC*) for rill-interrill erosion susceptibility models (RISMs), for both calibration (AUC_{train}) and validation (AUC_{test}) subsets, computed for the four subsets (S1|–S4).

Table 4. Area under the receiver operating characteristic curve (*AUC*) for gully erosion susceptibility models (GUSMs), for both calibration (AUC_{train}) and validation (AUC_{test}) subsets, computed for the four subsets (S5–S8).

Table 5. Accuracy statistics for the best data set and the whole basin, for both RISM and GUSM.

ACCEPTED MANUSCRIPT

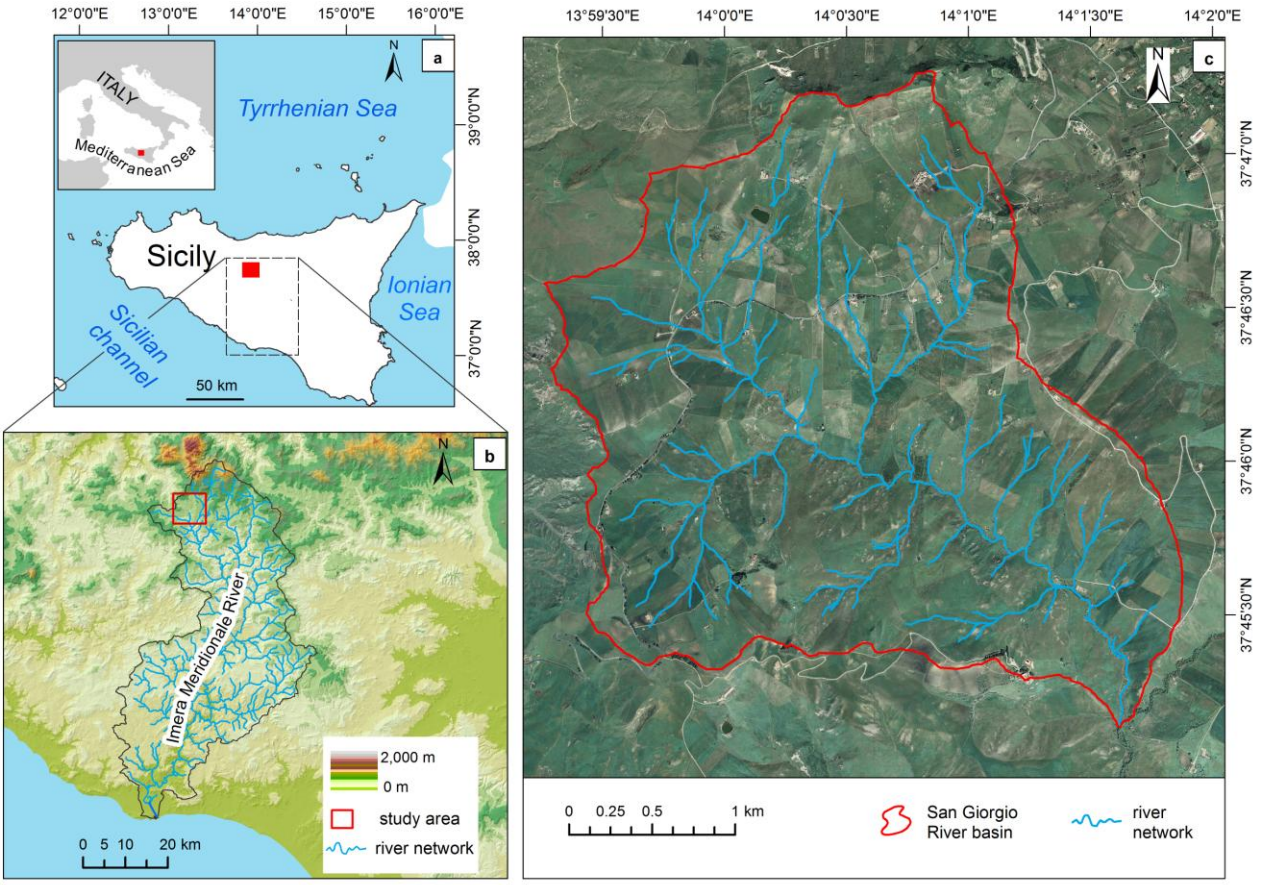

Figure 1

ACCEPTED

ACCEPTED MANUSCRIPT

Figure 2

ACCEPTED MANUSCRIPT

ACCEPTED MANUSCRIPT

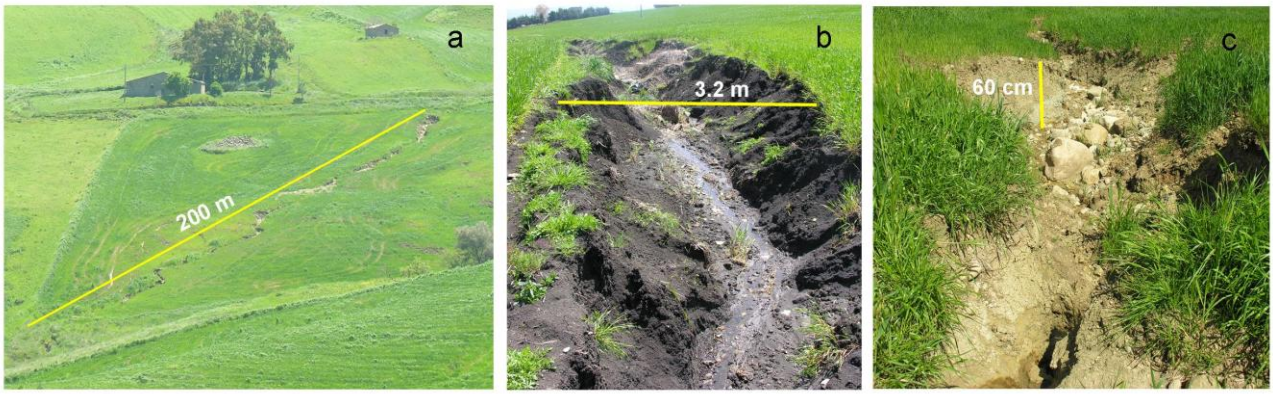

Figure 3

ACCEPTED MANUSCRIPT

ACCEPTED MANUSCRIPT

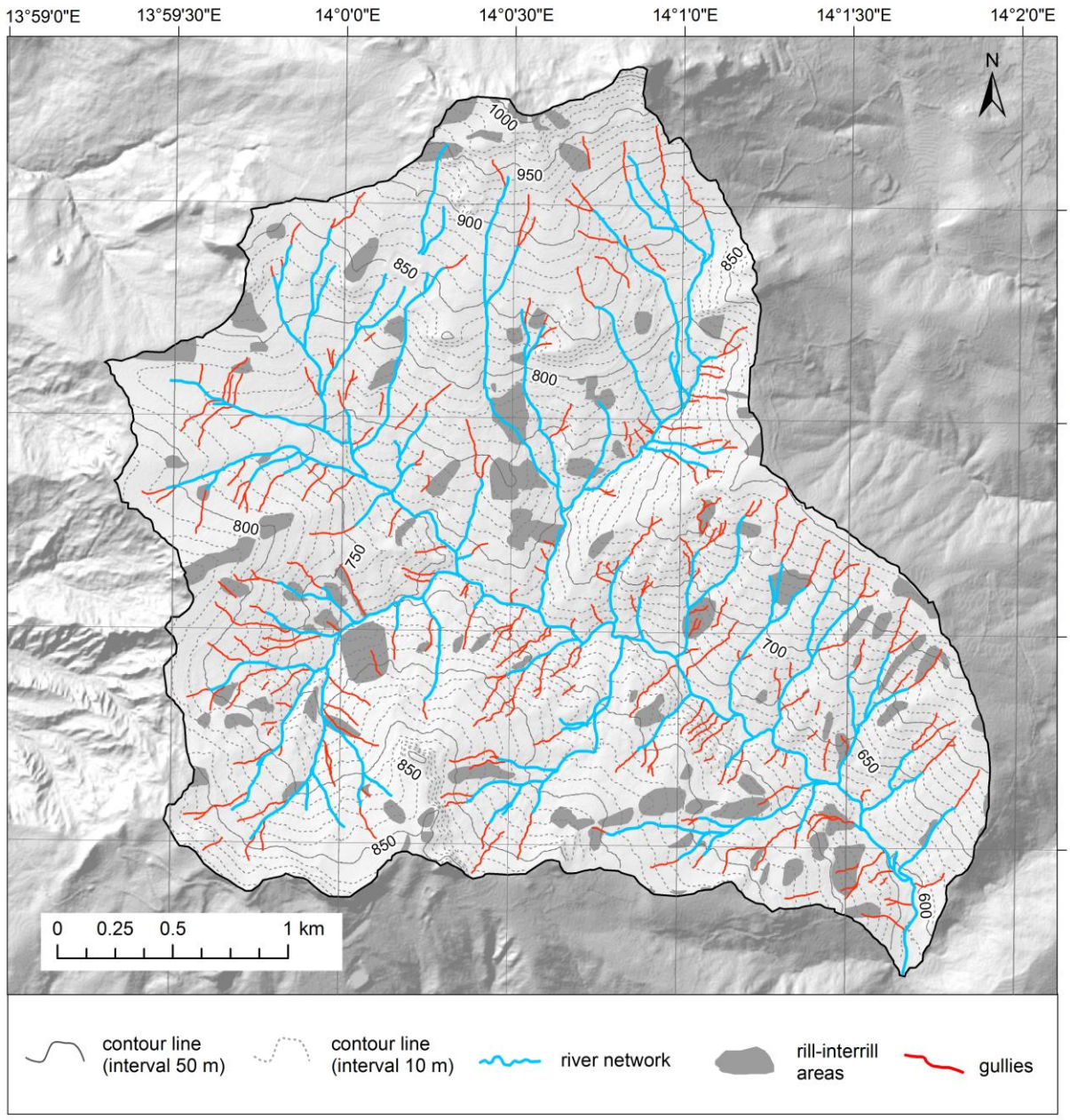

Figure 4

ACCEPTED MANUSCRIPT

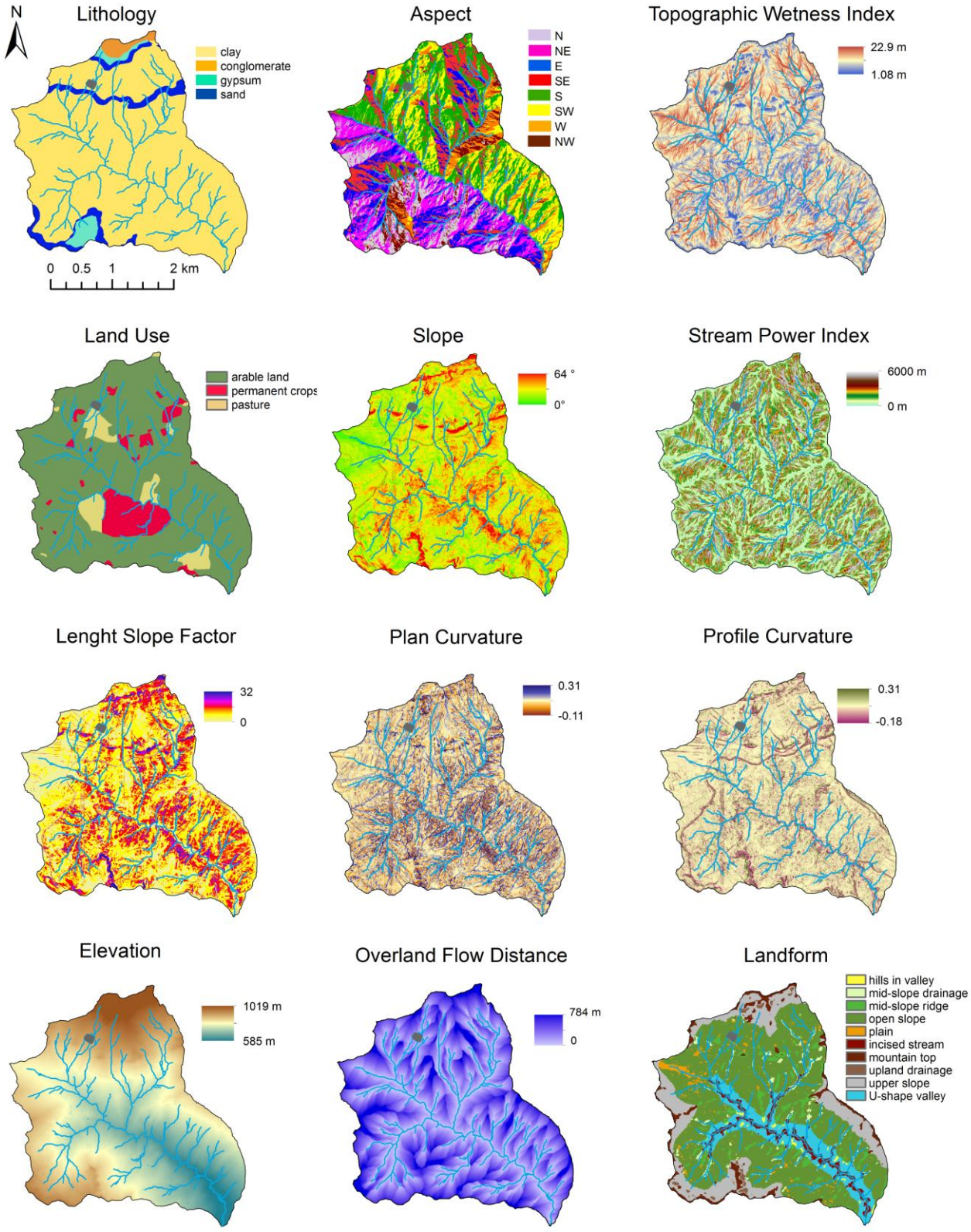

Figure 5

ACCEPTED MANUSCRIPT

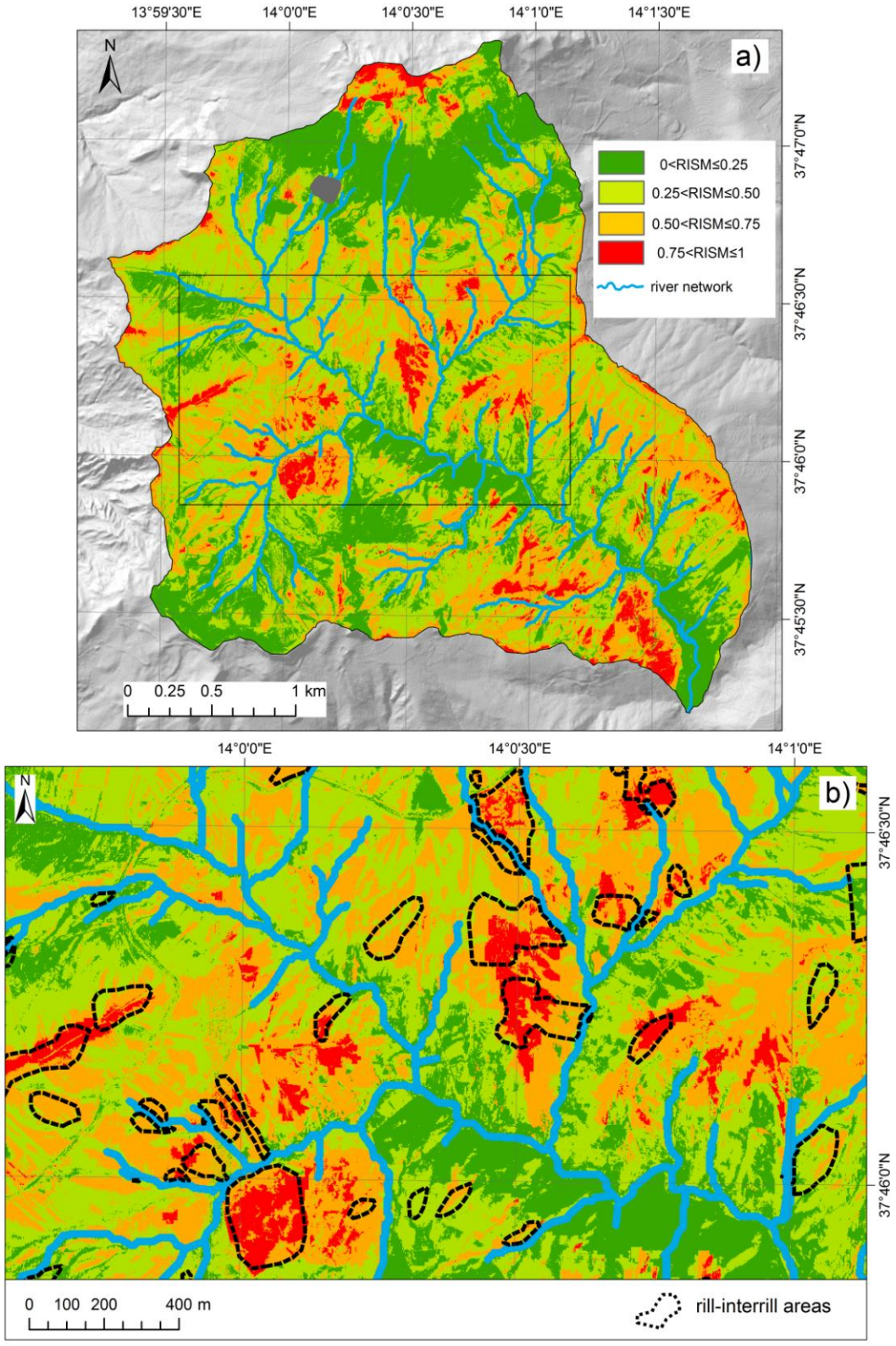

Figure 6

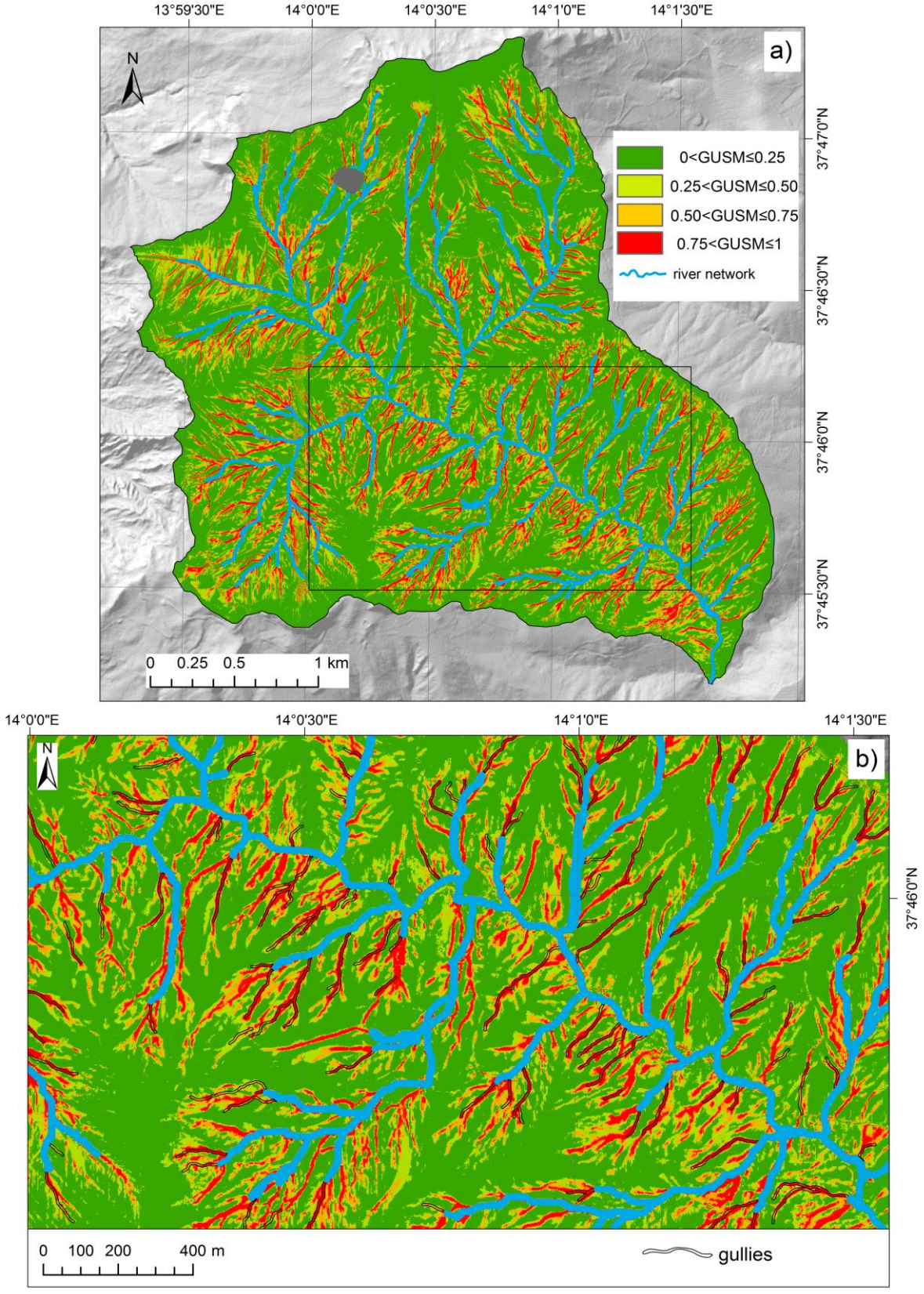
13°59'30"E
14°0'0"E
14°0'30"E
14°1'0"E
14°1'30"E
a)
N
0<GUSM≤0.25
0.25<GUSM≤0.50
0.50<GUSM≤0.75
0.75<GUSM≤1
river network
37°47'0"N
37°46'30"N
37°46'0"N
37°45'30"N
0 0.25 0.5 1 km
14°0'0"E
14°0'30"E
14°1'0"E
14°1'30"E
b)
N
37°46'0"N
0 100 200 400 m
gullies

Figure 7

ACCEPTED MANUSCRIPT

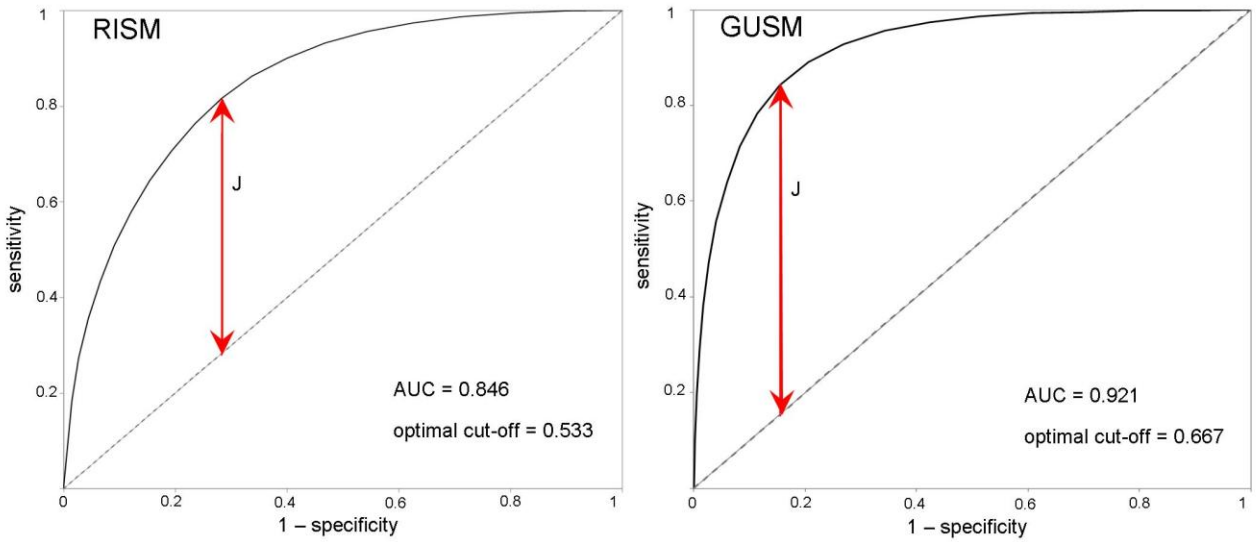

Figure 8

ACCEPTED MANUSCRIPT

ACCEPTED MANUSCRIPT

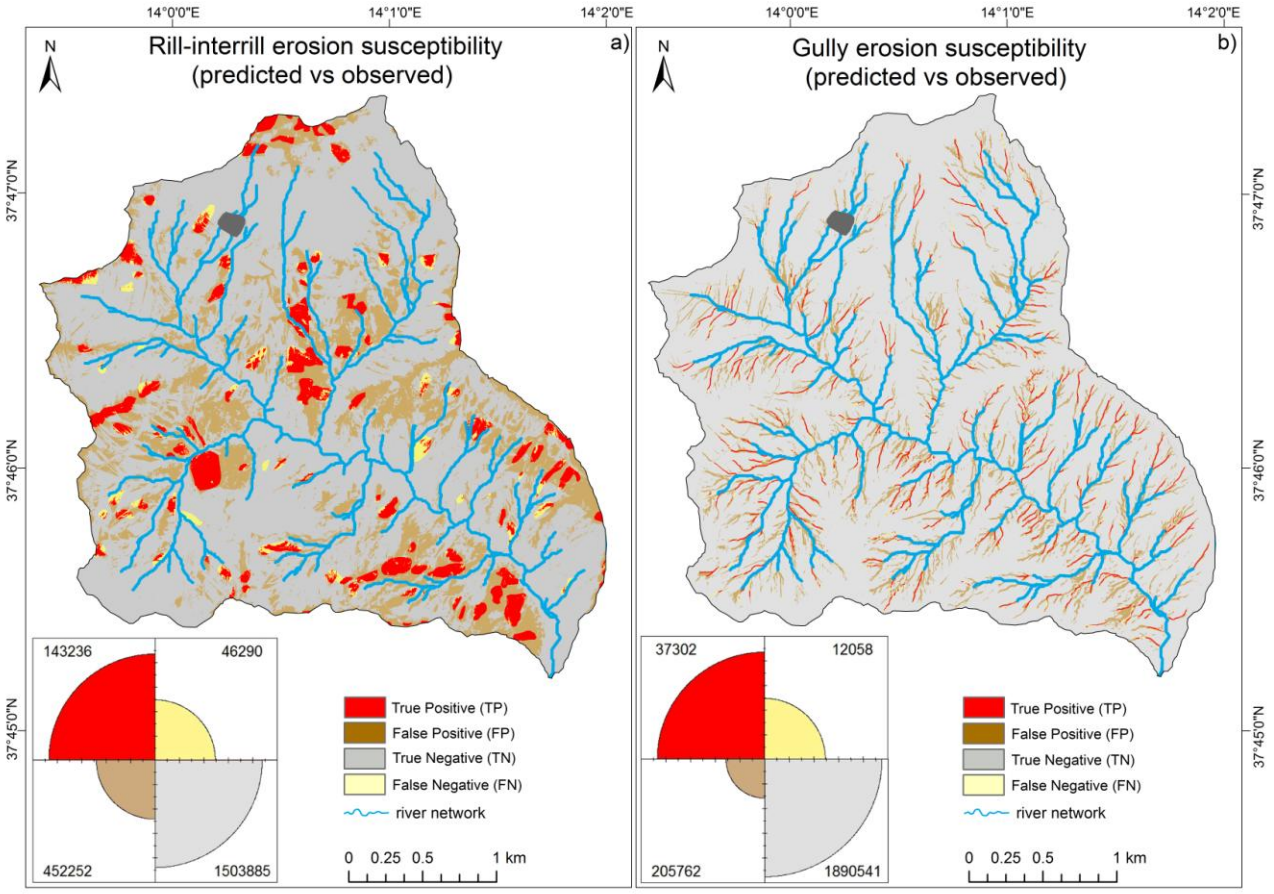

Figure 9

ACCEPT

ACCEPTED MANUSCRIPT

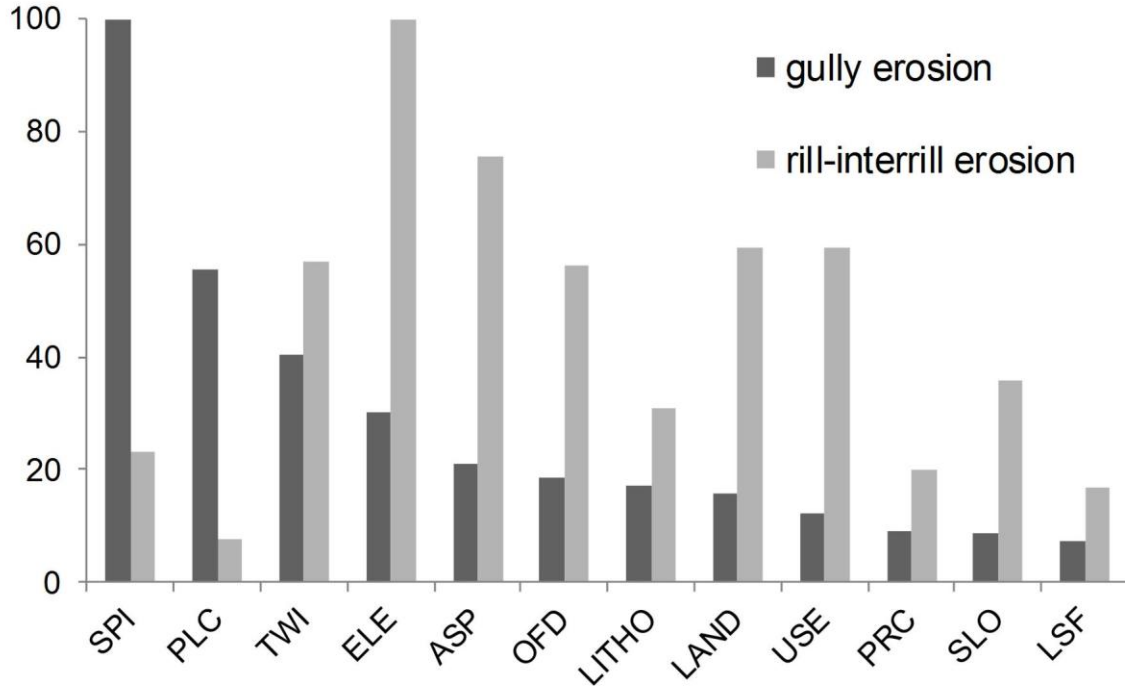

Figure 10

ACCEPTED MANUSCRIPT

ACCEPTED MANUSCRIPT

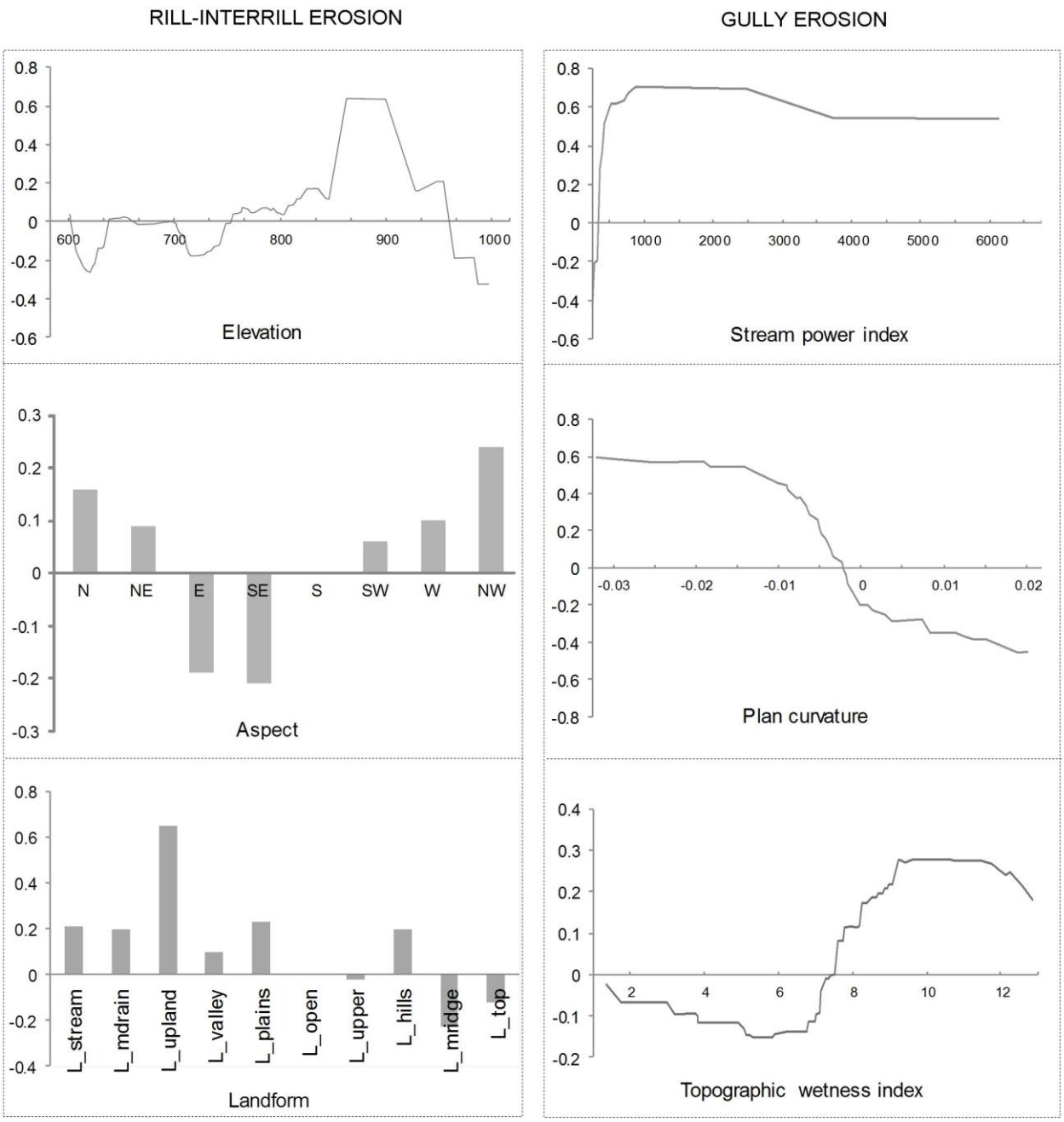

Figure 11

ACCEPTED MANUSCRIPT

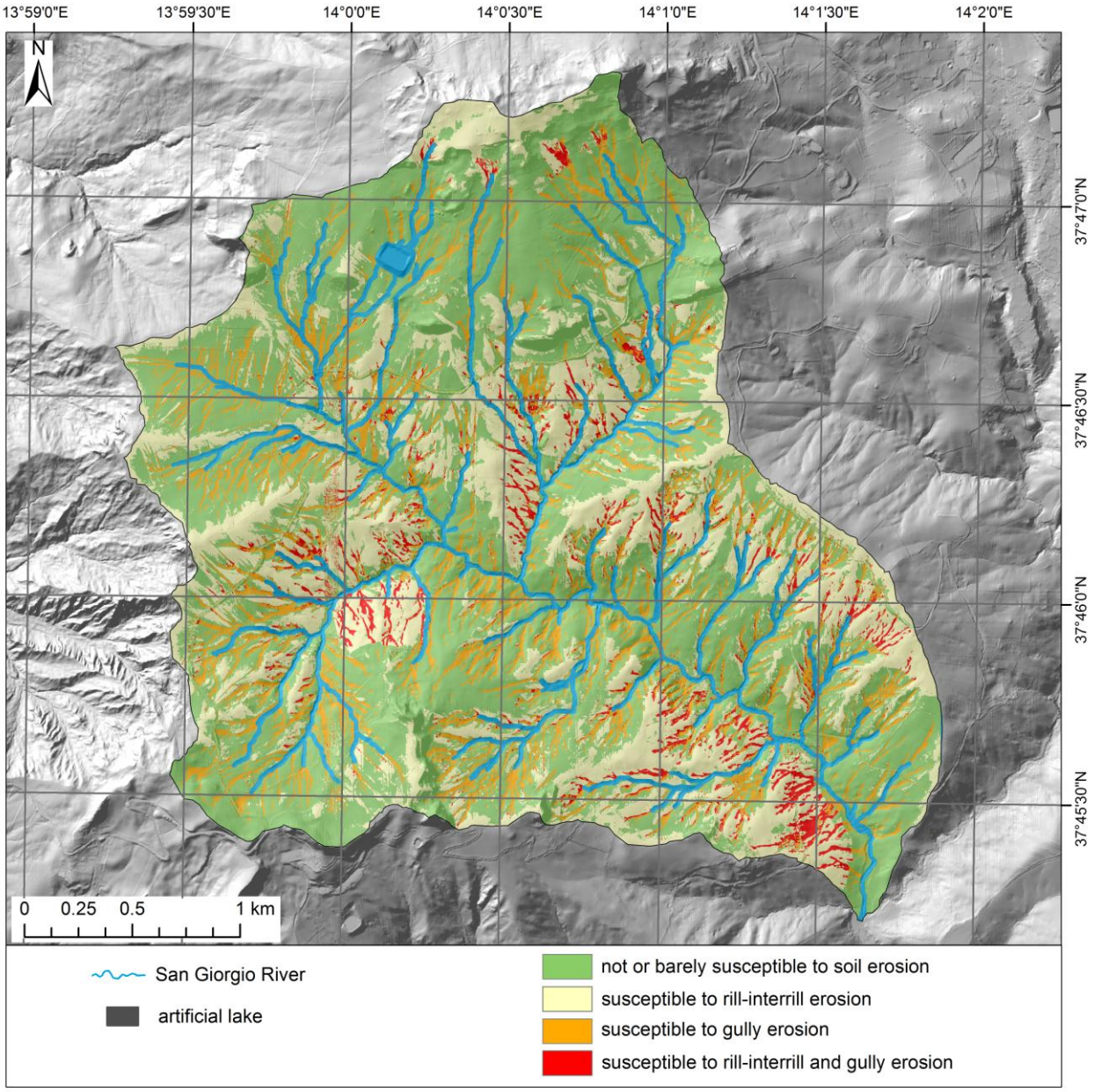

Figure 12

ACCEPTED MANUSCRIPT

Table 1

Discrete variable		code	%
Lithology (LITHO)	clay	LTL_clay	62.6
	conglomerate	LTL_cong	17.2
	gypsum	LTL_gyps	14.2
	sandstone	LTL_sand	6.0
Land use (USE)	arable land	USE_arable	81.2
	permanent crops	USE_crop	10.3
	pastures	USE_pasture	8.5
Aspect (ASP)	north	ASP_N	9.7
	north-east	ASP_NE	11.8
	east	ASP_E	11.8
	south-east	ASP_SE	13.4
	south	ASP_S	16.1
	south-west	ASP_SW	15.9
	west	ASP_W	12.1
	north-west	ASP_NW	9.2
Landform (LAND)	open slopes	L_open	56.5
	upper slopes	L_upper	16.5
	U-shape valleys	L_valley	10.2
	mid-slope ridges	L_mridge	4.5
	mountain tops	L_top	4.3
	deeply incised streams	L_stream	2.7
	plains	L_plains	2.2
	mid-slope drainages	L_mdrain	1.9
	upland drainages	L_upland	0.8
	hills in valleys	L_hills	0.5

ACCEPTED MANUSCRIPT

ACCEPTED MANUSCRIPT

Table 2

Continuous variable	code	unit	mean	std. dev.
Length-slope factor	*LSF*	none	2.5	1.4
Topographic wetness index	*TWI*	[m]	6.6	1.4
Stream power index	*SPI*	[m]	121.4	5016
Plan curvature	*PLC*	[rad^{-1}]	0.001	0.008
Profile curvature	*PRC*	[rad^{-1}]	0.0001	0.009
Elevation	*ELE*	[m a.s.l.]	770.9	78.3
Distance to the river	*OFD*	[m]	209.3	132.2
Slope angle	*SLO*	[°]	11.4	5.2

ACCEPTED MANUSCRIPT

ACCEPTED MANUSCRIPT

Table 3

RISM	S1	S2	S3	S4
AUC_{train}	0.847	0.848	0.837	0.830
AUC_{test}	0.846	0.846	0.830	0.822

ACCEPTED MANUSCRIPT

ACCEPTED MANUSCRIPT

Table 4

GUSM	S5	S6	S7	S8
AUC_{train}	0.926	0.922	0.900	0.873
AUC_{test}	0.921	0.920	0.890	0.867

ACCEPTED MANUSCRIPT

ACCEPTED MANUSCRIPT

Table 5

	RISM		GUSM	
	Test dataset	Whole basin	Test dataset	Whole basin
Sensitivity *TP*/(*TP*+*FN*)	0.81	0.76	0.84	0.76
Specificity *TN*/(*FP*+*TN*)	0.73	0.77	0.85	0.90
1-precision 1-(*TP*/(*TP*+*FP*)	0.25	0.76	0.15	0.85
Negative predictive value *TN*/(*TN*+*FN*)	0.79	0.97	0.84	0.99
Accuracy (*TP*+*TN*)/(*FP*+*FN*)	0.77	0.77	0.85	0.90

ACCEPTED MANUSCRIPT

ACCEPTED MANUSCRIPT

Highlights

- *We explore the ability of Stochastic Gradient Treeboost in predicting the spatial occurrence of rill-interrill and gully erosion;*
- *The overall accuracy of the susceptibility models is excellent;*
- *The relationships between erosion processes and predictors is analyzed;*
- *We design a methodological approach to create combined erosion susceptibility maps.*

ACCEPTED MANUSCRIPT